Robert H. Cleveland
Edward Y. Lee
Editors

Imaging in Pediatric Pulmonology

Second Edition

Springer

Imaging in Pediatric Pulmonology

Robert H. Cleveland • Edward Y. Lee
Editors

Imaging in Pediatric Pulmonology

Second Edition

Springer

Editors
Robert H. Cleveland
Department of Radiology
Harvard Medical School Boston Children's Hospital
Boston, MA
USA

Edward Y. Lee
Department of Radiology
Harvard Medical School Boston Children's Hospital
Boston, MA
USA

ISBN 978-3-030-23978-7 ISBN 978-3-030-23979-4 (eBook)
https://doi.org/10.1007/978-3-030-23979-4

This Springer imprint is published by the registered company Springer Nature Switzerland AG
The registered company address is: Gewerbestrasse 11, 6330 Cham, Switzerland

Foreword

In pediatric radiology, whether in academic medical centers, or in private practice, the chest is the most frequently imaged part of the entire body. Millions of chest radiographs are taken across the country on infants and children, and read by radiologists of all levels of training, both in hospital and outpatient imaging sites. Adult radiologists are often called upon to read chest images from emergency departments or neonatal intensive care units. Most pediatric radiologists spend hours each week reading chest images, a task they will do their entire careers. As a result, having a well-grounded knowledge of pulmonary imaging in pediatrics is imperative for all image interpreters.

This updated text has taken on the challenge of providing this education. In the second edition of the book, *Imaging in Pediatric Pulmonology*, the authors cater to all possible readers. For general radiologists looking to enhance their knowledge of pediatric lung conditions, extensive information on neonatal conditions, pneumonia, and common diseases abounds. For pediatric radiologists who want to learn about rarer conditions, like plastic bronchitis, or who want to deepen their understanding of the complexities of pediatric pulmonary disease, chapters are there. The way in which the material is organized makes it easy to learn about conditions in a variety of ways. Cystic fibrosis, for instance, is discussed in its own chapter, but also in chapters on focal lung disease, interstitial lung disease, airway abnormalities, genetic lung conditions, lung transplantation, and others. This distribution of material throughout the book into carefully chosen disciplines allows readers with a specific bent to learn about disease processes in their contexts of interest.

Additionally, the authors have given readers detailed information about areas not typically covered. A whole chapter is dedicated to pleural effusions and pneumothoraces. Pulmonary lymphatic disorders, venous drainage conditions, pulmonary embolism, even "incidentalomas" – the list goes on and on. In this broad and extensive survey of pediatric lung diseases, the authors have truly provided a comprehensive reference that should be included in any radiology library.

Dr. Robert H. Cleveland, whose career has been dedicated to pulmonary imaging, both at Massachusetts General Hospital and Boston Children's Hospital, by this work, continues to enhance his legacy. The addition of Dr. Edward Y. Lee, a colleague at Boston Children's Hospital, and an acclaimed author and speaker on pediatric lung imaging, only adds to the prestige of this book. New images, new techniques, and new explanations abound throughout the revised text. Truly, reviewing this updated addition to *Imaging in Pediatric Pulmonary*, was an honor and an education.

Atlanta, GA, USA

Stephen F. Simoneaux, MD, FACR

Preface

Since the publication of the prior edition of this book, many advances have occurred in the performance of computed tomography (CT) and magnetic resonance imaging (MRI). For CT, examination performance times have diminished significantly, greatly enhancing the ability to perform CT on unsedated children. Possibly more important to pediatric practice, the radiation doses of CT have been significantly reduced. However, the concern of lifetime exposure to ionizing irradiation remains paramount, and therefore, the use of CT should be limited to instances where no other viable choice is available. MRI procedure times have also been shortened and resolution improved. Although this makes MRI a viable alternative or preferable imaging choice for questions of larger structures such as the central airway, cardiovascular system, lung parenchyma, and chest wall, it is still not able to accurately depict the smaller airways.

Consequently, this new edition again focuses on plain film imaging as well as advanced imaging. The material, in some instances, has been reorganized. In addition, there are three new chapters specifically addressing pediatric pulmonary embolism, thoracic MRI, and the genetics of pediatric pulmonary disorders.

The overall organization of the book remains the same with an initial chapter of clinical algorithms for the most common clinical scenarios presenting to pediatric pulmonologists or pediatricians. The branch points in the algorithms serve as references to diseases discussed elsewhere in the book. There are again several chapters dedicated to specific topics such as lung transplantation and fetal imaging.

Rather than assuming a priori knowledge or suspicion of the diagnosis, this text can lead the reader to a differential diagnosis based on clinical parameters and thus direct reading to the relevant diagnoses. If the readers know their topic of interest, the chapters are organized for easy access to a broad range of abnormalities. While radiologists may find this a new approach in organization of a textbook, clinicians hopefully find it a “user-friendly” imaging resource.

I would be remiss if I did not acknowledge, with much gratitude, the encouragement and assistance of the members of the New England Pulmonary Consortium who have been so much a part of my development as a pediatric pulmonary imager over the almost 40 years of our association.

Boston, MA, USA — Robert H. Cleveland

Acknowledgments

For this, the second edition of *Imaging in Pediatric Pulmonology*, I again would like to thank the members of the New England Pediatric Pulmonary Consortium for their nearly 40 years of friendship, teaching, and camaraderie. They have been the inspiration for this book.

Special thanks go to the many authors who have contributed to this second edition, both new and those who contributed previously. I am also deeply in debt to Dr. Ed Lee who has graciously provided his time and talent as coeditor for this edition.

The preparation of this edition has changed somewhat from the original textbook. As a part of this change, the editorial responsibilities have been assumed by my coeditor, Ed Lee, and myself. This does not diminish the tremendous gratitude I owe to the original associate editors, Claire Langston, Andrew Colin, and Ed Lee, or the assistant editor, Mei Mei Chow. I would also like to thank the several chapter authors of the original text who were not able to participate in this second edition.

Finally, I want to express sincere appreciation to all my clinical and imaging colleagues at the Massachusetts General Hospital and Boston Children's Hospital with whom it has been such a pleasure to work over the course of my career.

Bob Cleveland
Harvard Medical School
Boston, MA, USA
January 2019

Words cannot express my gratitude and appreciation to Dr. Bob Cleveland, a true pioneer in pediatric pulmonary imaging, who has been a main teacher and mentor for my career as an academic radiologist specialized in pediatric pulmonary imaging at Boston Children's Hospital.

Through this book, it is truly a great honor for me to be able to be a part of continuing Dr. Cleveland's lifelong dedication to academic radiology, enthusiasm for advancing the field of pediatric pulmonary imaging, and contribution to teaching and spreading his knowledge to others for pediatric patient care.

In addition, I would also like to acknowledge the trainees and clinicians that I have met during my academic career for sharing their enthusiasm for learning and the young patients of Boston Children's Hospital who always enlighten and remind us of the importance of advancing the field of pediatric pulmonary imaging.

Edward Y. Lee
Harvard Medical School
Boston, MA, USA
January 2019

Contents

Contributors

Mohammad Amarneh, MD Department of Pediatric and Interventional Radiology, University of Iowa Carver College of Medicine, Iowa City, IA, USA

Dorothy Bulas, MD Department of Diagnostic Imaging and Radiology, George Washington University Medical Center, Children's National Medical Center, Washington, DC, USA

Thomas Carraway, MD Department of Radiology, Maine Medical Center, Portland, ME, USA

Alicia Casey, MD Division of Pulmonary Medicine, Boston Children's Hospital, Harvard Medical School, Boston, MA, USA

Marilynn Chan, MD Department of Pediatric Pulmonology, University of California San Francisco Medical Center, San Francisco, CA, USA

Gulraiz Chaudry, MBChB, MRCP, FRCR Department of Radiology, Boston Children's Hospital and Harvard Medical School, Boston, MA, USA

Giuseppe Cicero, MD Department of Radiology and Nuclear Medicine, Sophia Children Hospital – Erasmus Medical Center, Rotterdam, The Netherlands

Department of Biomedical Sciences and Morphological and Functional Imaging, University of Messina, Messina, Italy

Pierluigi Ciet, MD, PhD Department of Radiology and Nuclear Medicine, Sophia Children Hospital – Erasmus Medical Center, Rotterdam, The Netherlands

Robert H. Cleveland, MD Department of Radiology, Harvard Medical School, Boston Children's Hospital, Boston, MA, USA

Anne C. Coates, MD Department of Pediatrics, Stanford School of Medicine/Lucille Packard Children's Hospital, Palo Alto, CA, USA

Andrew A. Colin, MD Miller School of Medicine, University of Miami, Miami, FL, USA

Alexia Egloff, MD Department of Radiology, Children's National Medical Center, Washington, DC, USA

Mary Shannon Fracchia, MD Department of Pediatric Pulmonary, Massachusetts General Hospital, Harvard Medical School, Boston, MA, USA

Charles K. Grimes, MD Department of Radiology, Maine Medical Center, Portland, ME, USA

Megan H. Hawley, MS, CGC Pediatric Pulmonary Division, Massachusetts General Hospital for Children, Boston, MA, USA

Monica Kahye Johnson, MD Department of Radiology, Harvard Medical School and Massachusetts General Hospital, Boston, MA, USA

Umakanth Katwa, MD Boston Children's Hospital and Harvard Medical School, Boston, MA, USA

T. Bernard Kinane, MD Pediatric Pulmonary Division, Massachusetts General Hospital for Children, Boston, MA, USA

Stella Kourembanas, MD Department of Newborn Medicine, Boston Children's Hospital, Boston, MA, USA

Katie Krone, MD Division of Pulmonary Medicine, Boston Children's Hospital, Harvard Medical School, Boston, MA, USA

Jason E. Lang, MD Division of Allergy, Immunology and Pulmonary Medicine, Duke University School of Medicine, Durham, NC, USA

Duke Children's Pulmonary Function Laboratory, Duke Clinical Research Institute, Duke Children's Health & Discovery Institute, Durham, NC, USA

Edward Y. Lee, MD, MPH Department of Radiology, Boston Children's Hospital and Harvard Medical School, Boston, MA, USA

Jonathan C. Levin, MD Department of Newborn Medicine and Respiratory Disease, Boston Children's Hospital, Boston, MA, USA

Mark C. Liszewski, MD Department of Radiology, Division of Pediatric Radiology, Montefiore Medical Center, Bronx, NY, USA

Raymond Liu, MD, FSIR Department of Radiology, Massachusetts General Hospital, Boston, MA, USA

Peter P. Moschovis, MD, MPH Pediatric Pulmonary Division, Massachusetts General Hospital for Children, Boston, MA, USA

Kara E. May, MD Department of Medicine, Division of Respiratory Diseases, Boston Children's Hospital and Harvard Medical School, Boston, MA, USA

Sanjay P. Prabhu, MBBS, FRCR Department of Radiology, Boston Children's Hospital and Harvard Medical School, Boston, MA, USA

Annabelle Quizon, MD Department of Respiratory Medicine, University of California San Diego- Rady Children's Hospital, San Diego, CA, USA

Dennis Rosen, MD Division of Pulmonary Medicine, Boston Children's Hospital and Harvard Medical School, Boston, MA, USA

Efraim Sadot, MD Department of Pediatric Intensive Care, Dana-Dwek Children's Hospital, Tel-Aviv Sourasky Medical Center and Sackler Faculty of Medicine, Tel-Aviv University, Tel Aviv-Yafo, Israel

Pallavi Sagar, MD Department of Radiology, Harvard Medical School and Massachusetts General Hospital, Boston, MA, USA

Ashraf Thabet, MD Department of Interventional Radiology, Massachusetts General Hospital, Harvard Medical School, Boston, MA, USA

Frédéric Thomas-Chaussé, MD FRCPC Department of Radiology, Radiation Oncology and Nuclear Medicine, University of Montreal, CHU Sainte-Justine, Montréal, QC, Canada

Gary Visner, DO Boston Children's Hospital, Harvard Medical School, Boston, MA, USA

Abbey J. Winant, MD, MFA Department of Radiology, Boston Children's Hospital and Harvard Medical School, Boston, MA, USA

Lael M. Yonker, MD Pediatric Pulmonary Division, Massachusetts General Hospital for Children, Boston, MA, USA

Clinical Algorithms

1

Dennis Rosen, Jason E. Lang, and Andrew A. Colin

Introduction

In medical practice, patients often present without a known diagnosis. Physicians move from a set of signs and symptoms to the formation of a differential diagnosis to a final diagnosis. This introductory chapter provides seven clinical algorithms that encompass a large part of the spectrum of pediatric pulmonary practice. By navigating through the appropriate algorithm, reference to possible relevant diagnoses may be encountered which will provide direction to further reading in the textbook.

The algorithms are as follows:

- Chest pain
- Chronic cough
- Cyanosis/hypoxia
- Shortness of breath
- Airway bleeding
- Noisy breathing
- Tachypnea

Chest Pain

See Fig. 1.1.

Chronic Cough

See Fig. 1.2.

Cyanosis and Hypoxia

Cyanosis is often associated with hypoxia, but the two do not always coexist (Fig. 1.3). *Acrocyanosis* is commonly associated with vasoconstriction, whereas *central cyanosis* is most often found in the perioral area and is reflective of at least 5 g/% of unsaturated hemoglobin. This can result from different causes, which will be reviewed systematically. In general, it is helpful to consider the causative mechanism of the cyanosis. These different mechanisms may include:

- Shunting of *blue* deoxygenated blood from the venous circulation to the arterial circulation, bypassing the alveolar capillary network
- Intrapulmonary shunting
- Ventilation/perfusion (V/Q) mismatching
- Inadequate ventilation
- Inadequate gas exchange at the level of the alveolus (diffusion defects)
- Inadequate bonding of O_2 to the red blood cells (hematologic causes)
- Inadequate perfusion

Shunting of blood can occur on many levels, primarily the heart, lung, and peripheral circulation. Cardiac causes may include cardiac malformations with right-to-left shunting, including primary heart lesions with right-to-left shunting (tetralogy of Fallot, transposition of great arteries, truncus arteriosus, pulmonic stenosis/atresia, aortic stenosis, Ebstein's anomaly, and hypoplastic left heart), and with lesions associated with pulmonary hypertension (either primary or secondary to increased pulmonary flow such as in Eisenmenger's syndrome), persistent fetal circulation, breath holding, and shunting through a patent foramen ovale.

D. Rosen (✉)
Division of Pulmonary Medicine, Boston Children's Hospital and Harvard Medical School, Boston, MA, USA
e-mail: Dennis.Rosen@childrens.harvard.edu

J. E. Lang
Division of Allergy, Immunology and Pulmonary Medicine, Duke University School of Medicine, Durham, NC, USA

Duke Children's Pulmonary Function Laboratory, Duke Clinical Research Institute, Duke Children's Health & Discovery Institute, Durham, NC, USA

A. A. Colin
Miller School of Medicine, University of Miami, Miami, FL, USA

R. H. Cleveland, E. Y. Lee (eds.), *Imaging in Pediatric Pulmonology*, https://doi.org/10.1007/978-3-030-23979-4_1

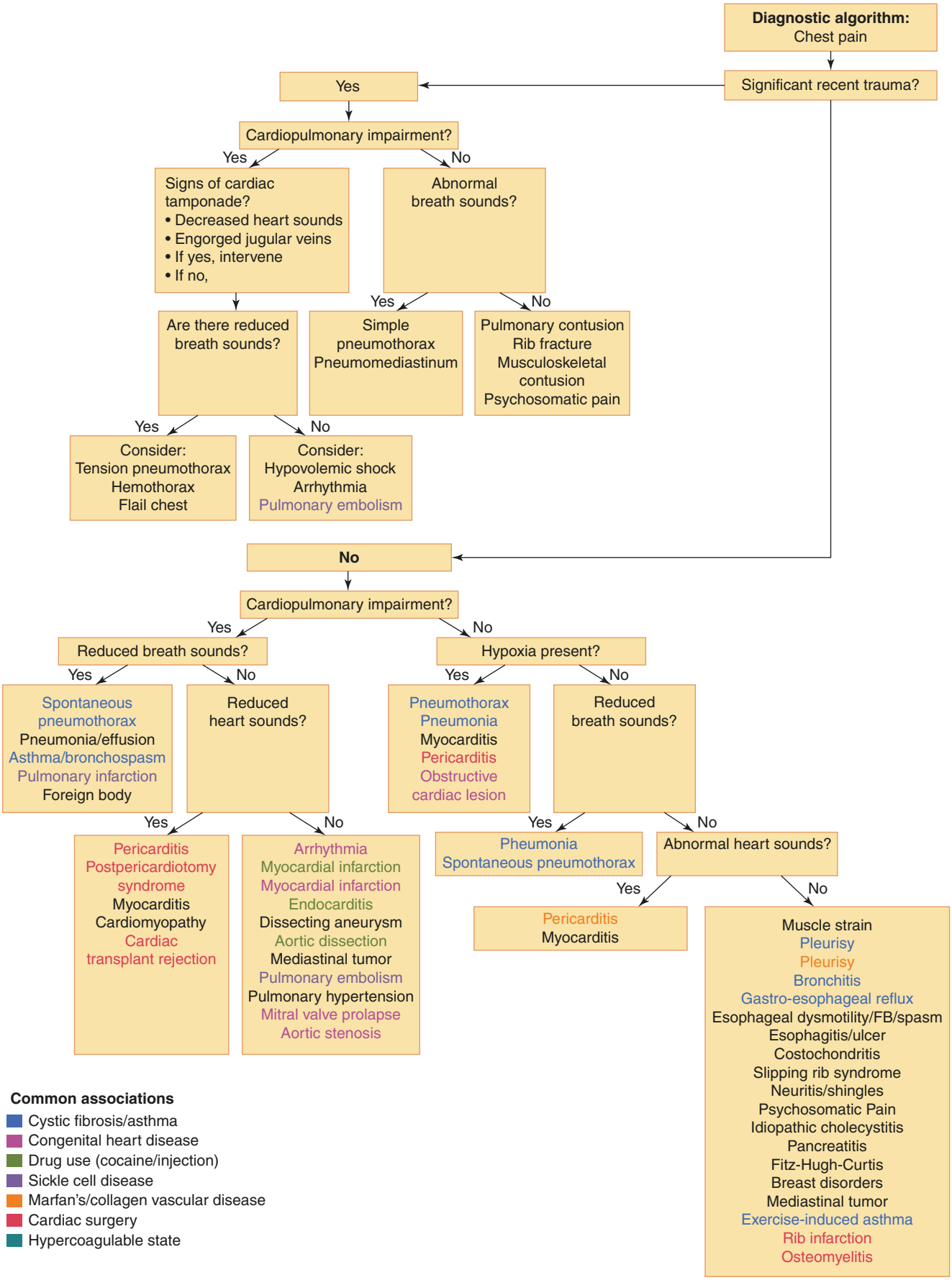

Fig. 1.1 Chest pain

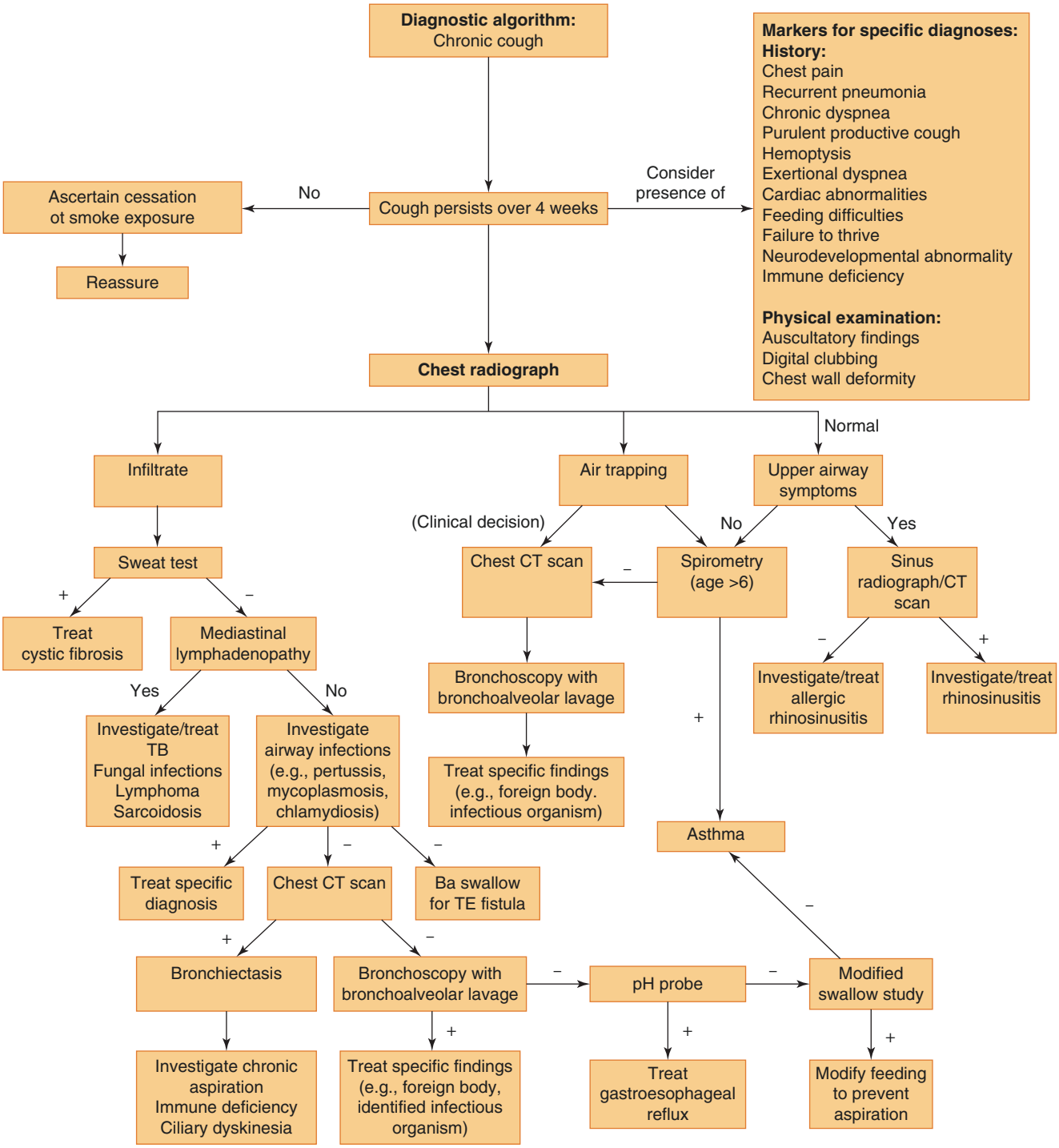

Fig. 1.2 Chronic cough

V/Q mismatching, in which there is good perfusion of under-ventilated lung, may occur with foreign body aspiration, in mucus plugging, atelectasis, in pneumonia with a large infiltrate, bronchiolitis, and pulmonary hemosiderosis. It is seen in cases of arteriovenous malformations (AVM), either primary or in the setting of liver failure and the hepatopulmonary syndrome. It can also be seen in restrictive lesions such as pneumothorax, pleural effusion, pulmonary fibrosis, pulmonary hemosiderosis, meconium aspiration, and respiratory distress syndrome (RDS) in neonates.

At the other end of the V/Q mismatching spectrum, in which there is under-perfusion of well-ventilated lung, may be found pulmonary emboli, pulmonary hypertension, and hyperinflative states such as asthma, bronchiolitis, and congenital lobar emphysema.

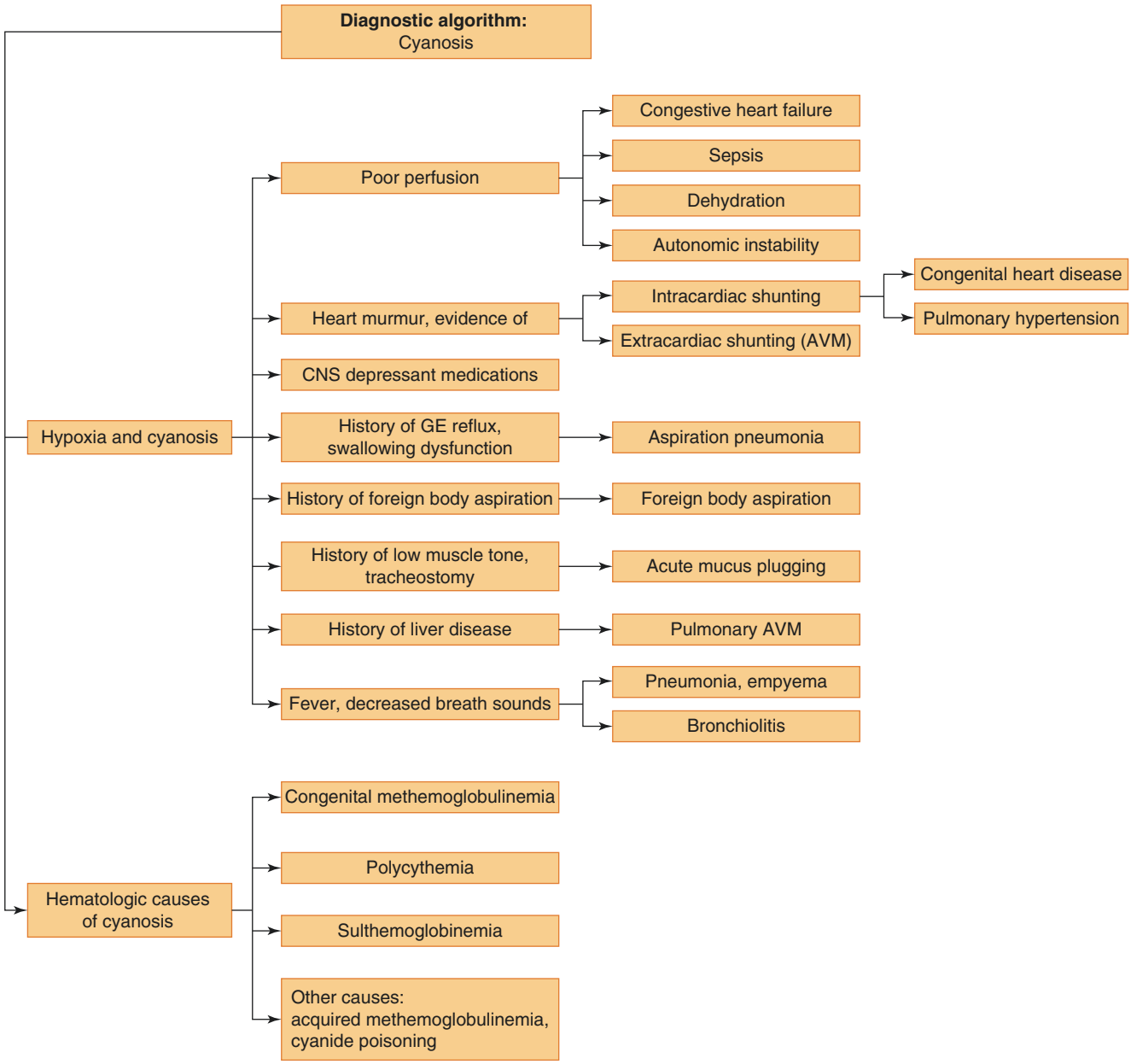

Fig. 1.3 Cyanosis

Inadequate ventilation may also result from restrictive defects such as pneumothorax, ribcage abnormalities, scoliosis, kyphosis, abdominal distention, and obesity, central control of breathing disorders such as congenital alveolar hypoventilation syndrome, and neuromuscular diseases such as muscular dystrophy, Werdnig–Hoffman, diaphragmatic paralysis, polio, and Guillain Barré. Obstructive processes such as nasal obstruction, retropharyngeal abscesses, tonsillar hypertrophy, severe croup, laryngeal webs, foreign body aspiration, obstructive sleep apnea, and hypoventilation syndrome. CNS depressant medications may also inhibit the respiratory drive.

Diffusion defects are caused by interstitial processes such as interstitial lung disease (ILD), bronchopulmonary dysplasia (BPD), pulmonary edema, hypersensitivity pneumonitis, and adult respiratory distress syndrome (ARDS).

Hematologic causes of cyanosis may include methemoglobinemia, either acquired (medication or nitrite ingestion) or congenital, polycythemia, and sulfhemoglobinemia. These are nonhypoxemic and can be distinguished by measurement of blood PaO_2 levels.

Poor perfusion leading to cyanosis may be cardiac in origin, stemming from congestive heart failure (primary, postischemia, secondary to myocarditis, arrhythmias, heart block, and pericarditis) or systemic causes, including shock, sepsis, autonomic instability, and medication effect.

Shortness of Breath

See Fig. 1.4.

Airway Bleeding

See Fig. 1.5.

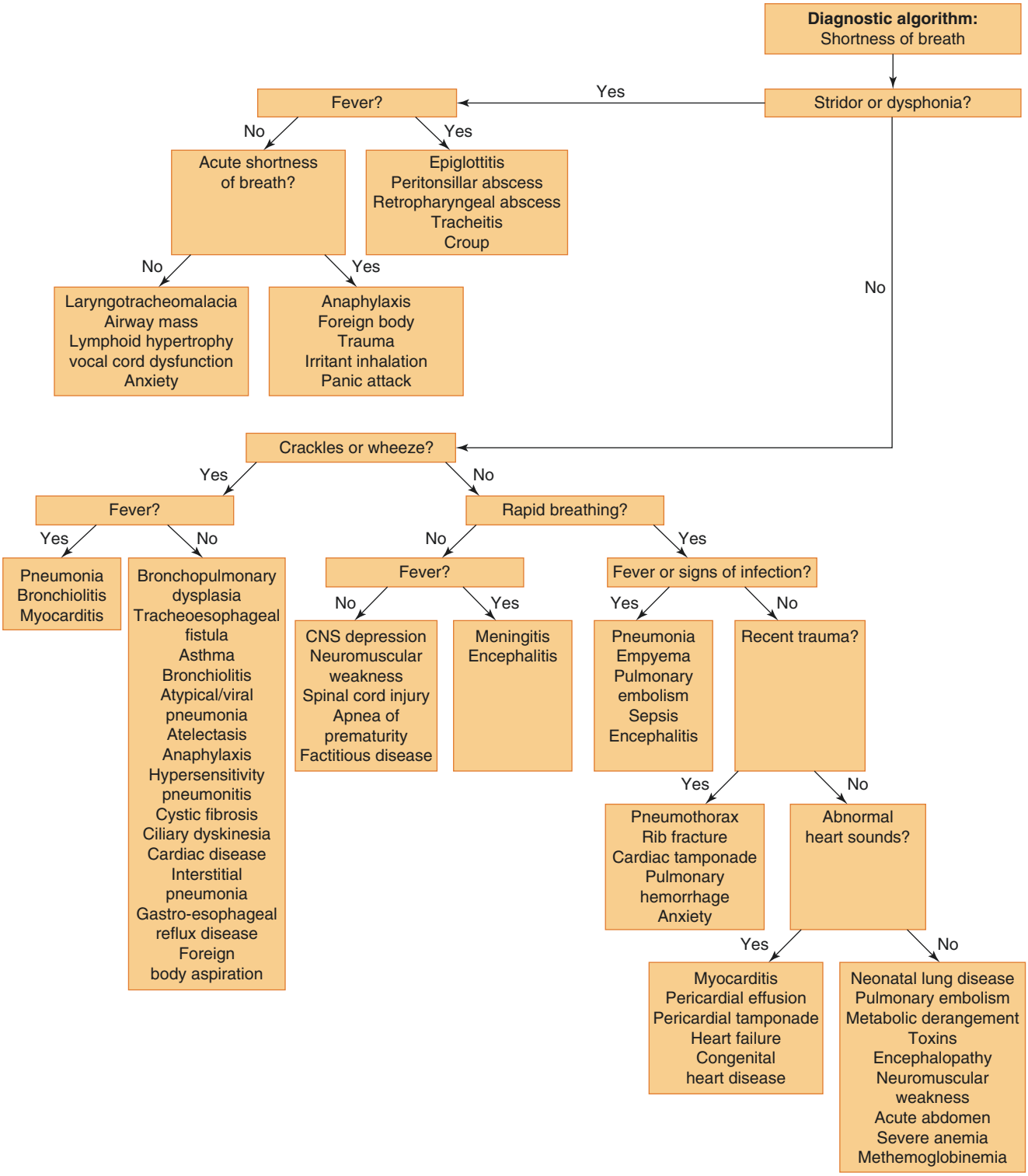

Fig. 1.4 Shortness of breath

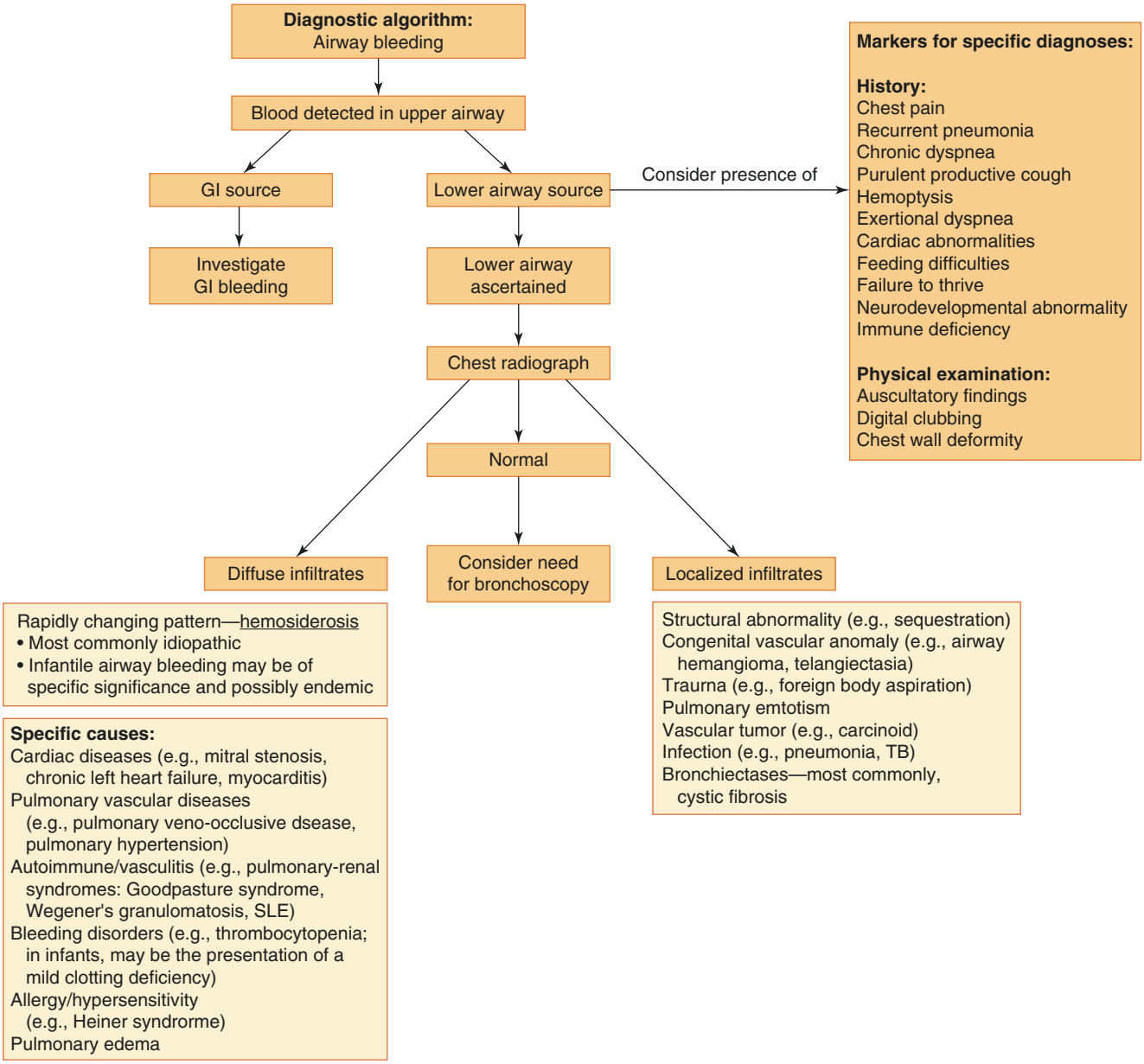

Fig. 1.5 Airway bleeding

Noisy Breathing

See Fig. 1.6a–c.

Tachypnea

Tachypnea is defined as a respiratory rate above the age-appropriate range, measured while the child is at rest (Fig. 1.7). The emphasis on age appropriateness is important, as infants may have resting respiratory rates ranging 30–60 breaths per minute, whereas children over the age of 2 will generally have resting respiratory rates ranging between 16 and 24 breaths per minute. This may be explained by a variety of factors, principal among which is the relatively high chest wall compliance of infants and toddlers, which decreases as children advance in age. Tachypnea may be a sign of an underlying disorder and in most cases represents an attempt by the body to improve gas exchange. It is detrimental as it results in increased energy expenditure, thus diverting calories away from other tasks such as growth. It may result in metabolic derangements, such as hyperventilation and respiratory alkalosis, and is difficult to sustain for a prolonged period of time because of progressive muscle fatigue. When caring for a child with tachypnea, it is important to identify and treat the underlying cause so as to prevent progression to respiratory failure.

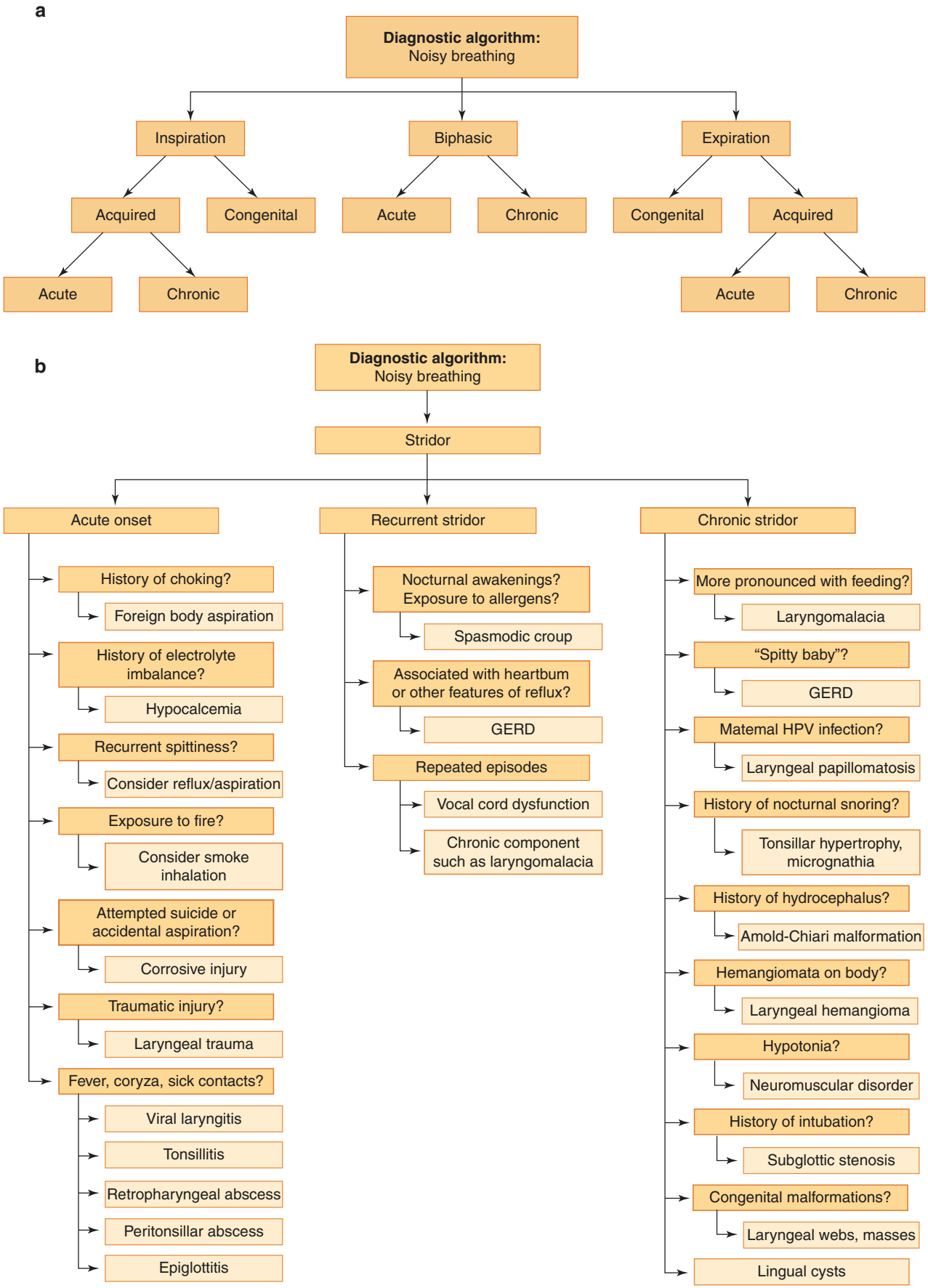

Fig. 1.6 Noisy breathing

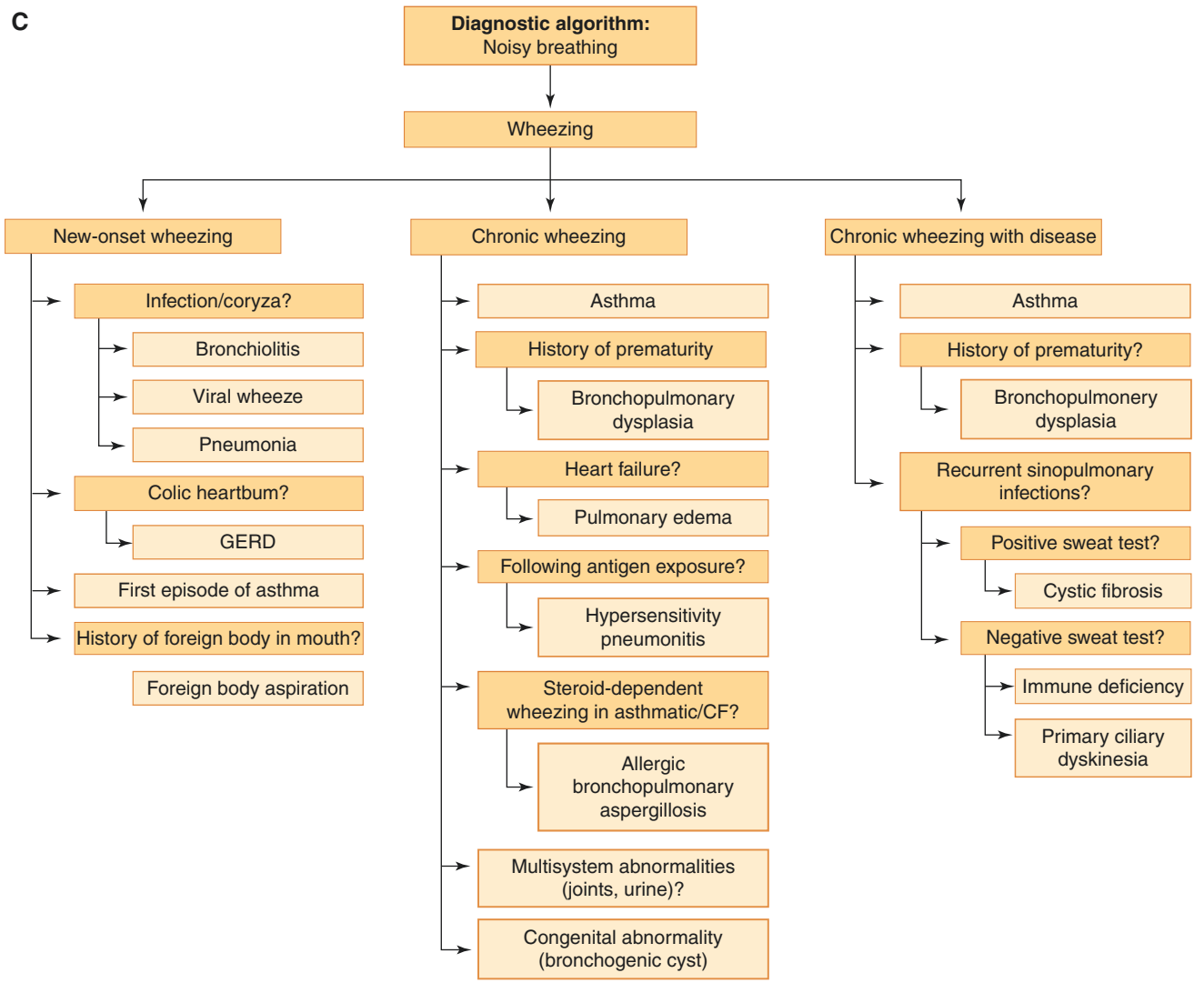

Fig. 1.6 (continued)

Causes of Tachypnea

There is a broad differential diagnosis for a child with tachypnea, encompassing not just pulmonary causes but also systemic, psychological, neurological, cardiac, and metabolic causes which are, for the most part, beyond the purview of this book.

Psychological

Emotional stress or anxiety can provoke tachypnea, often accompanied by hyperventilation, sometimes resulting in metabolic alkalosis and tetany.

Systemic

Pain and fever are both non-pulmonary causes of tachypnea. Poor perfusion accompanied by hypotension (such as in the case of dehydration or sepsis) can also lead to tachypnea, both as a compensatory mechanism to correct developing metabolic acidosis and as an attempt to improve oxygen delivery to end organs and tissues.

Metabolic

Both hypoxia and hypercarbia can increase the respiratory drive. Hypoxia may result from a decrease in the partial pressure of inspired oxygen, such as occurring at high altitudes, or from one or more of many pulmonary processes, which will be discussed shortly. Even when the intake and transport of oxygen are normal, in severe anemia, one can have a decrease in oxygen delivery to end organs and tissues and subsequently an increased respiratory rate.

There are many inborn errors of metabolism which can also bring about an increased basal respiratory rate, including urea cycle defects, methylmalonic acidemia, and isovaleric acidemia, to name but a few.

Acquired metabolic acidosis can induce hyperventilation with tachypnea as an attempt to correct the acidosis by increas-

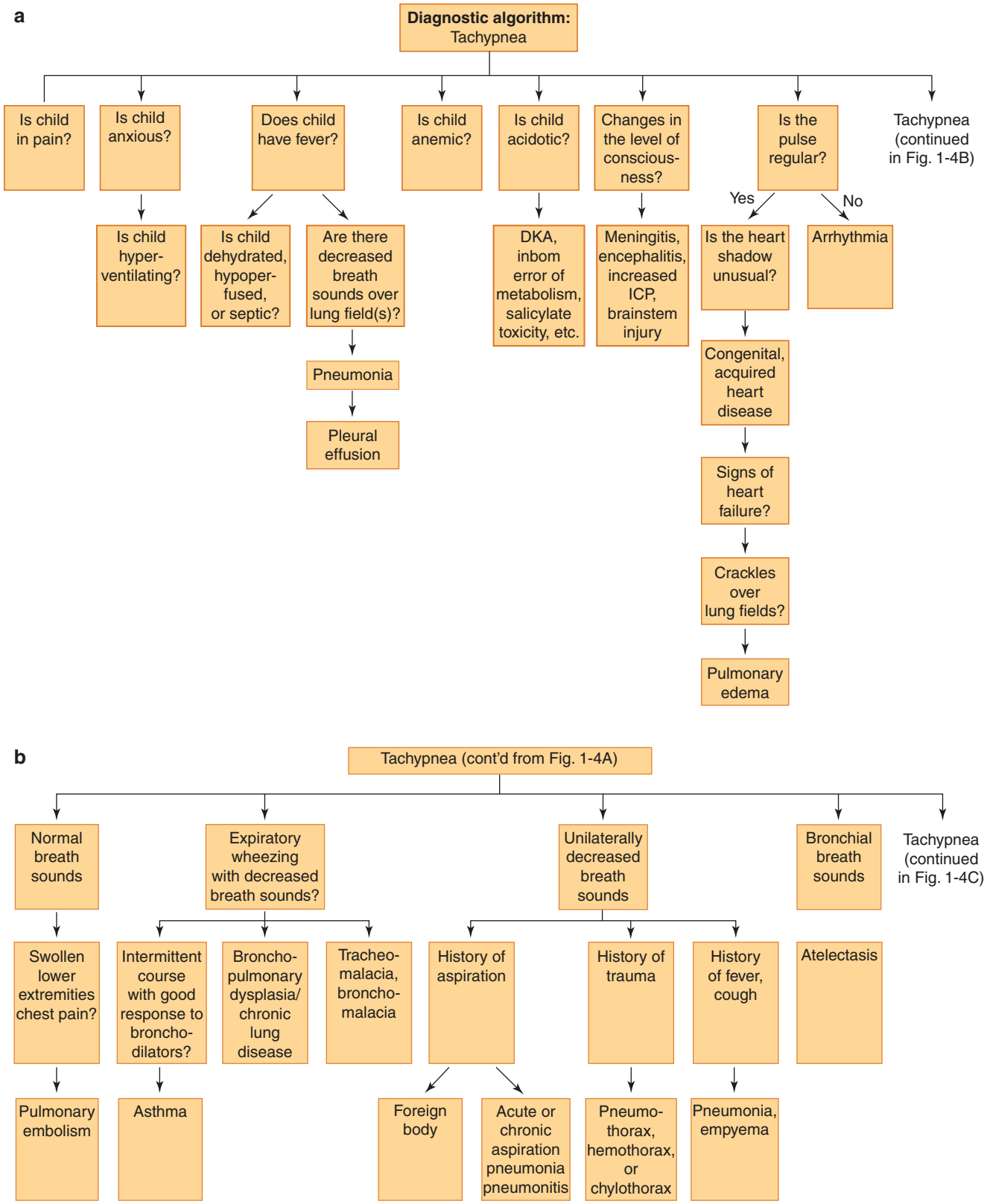

Fig. 1.7 Tachypnea

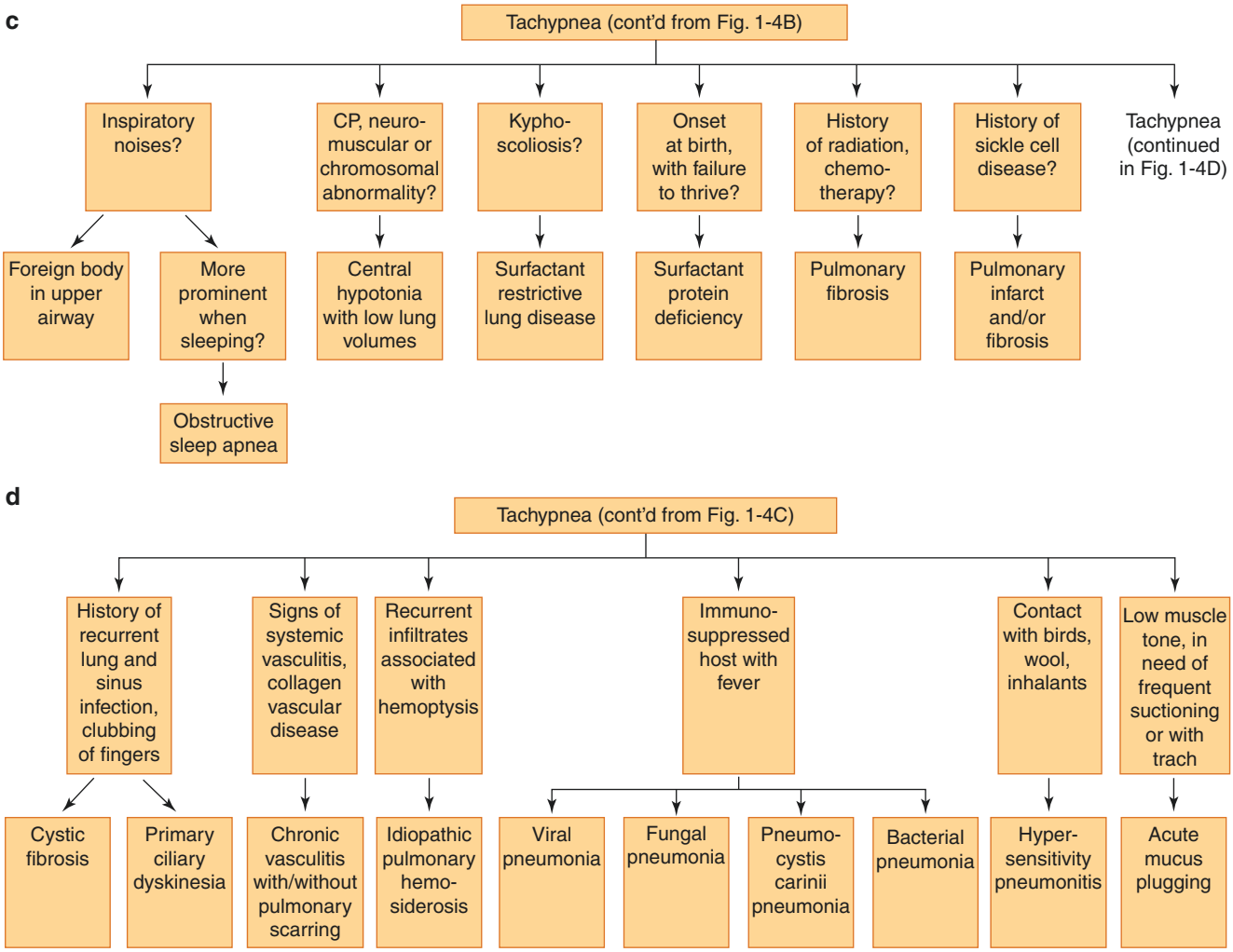

Fig. 1.7 (continued)

ing the clearance of CO_2 from the body, as described earlier. Causes of this include diabetic ketoacidosis, lactic acidosis, uremia, salicylate poisoning, dehydration, and sepsis.

Cardiac

Heart failure may cause tachypnea, either secondary to fluid accumulation in the lungs, such as in the case of pulmonary edema, or because of poor perfusion due to myocardial dysfunction. The presence of an irregular, weak, or rapid pulse, a murmur on physical exam, pulmonary edema, or an enlarged or abnormally shaped heart on chest X-ray should prompt a closer investigation of the heart and its function.

Neurological

Changes in intracranial pressure, encephalitis, and stroke are all recognized causes of tachypnea and should be considered in the context of the child's illness and presentation.

Pulmonary

Many types of pulmonary disease result in tachypnea because of a decrease in the proportion of tidal volume taking part in active gas exchange. In order to maintain minute ventilation, the respiratory rate needs to be increased. This can occur in obstructive processes, with air trapping; in restrictive processes, when the vital capacity is reduced, with the dead-space volume decreasing, remaining the same, or increasing; and in diffusion defects, when the amount of oxygen with any given breath traversing the alveolar membrane decreases. In cases of V/Q mismatching, such as pulmonary embolus, where tachypnea is one of the most common presenting signs, this is a result of the increase in functional dead space. Tachypnea also occurs in shunting, when a portion of the blood flow through the lungs is not exposed to the inspired air, resulting in hypoxemia, which in turn triggers a heightened respiratory drive.

Obstructive Processes

Obstructive processes can be subdivided into upper and lower airway obstruction, which refer to the location of the obstruction relative to the thoracic inlet. Examples of upper airway obstruction include acute laryngitis, foreign body aspiration, laryngomalacia, and obstructive sleep apnea. Lower airway obstruction may result from acute processes such as acute aspiration, or asthma exacerbation, and from chronic processes such as cystic fibrosis, bronchiectasis, bronchomalacia, tracheomalacia, BPD, chronic lung disease of prematurity, and chronic aspiration.

Restrictive Lung Disease

Restrictive lung disease may result from physical restriction of the lungs' capacity to insufflate, such as occurring chronically with kyphoscoliosis, neuromuscular disease, central hypotonia (in Down syndrome, Prader-Willi syndrome, other chromosomal disorders, and cerebral palsy), meningomyelocele, and congenital chest wall abnormality. It can be the result of an acute process that leads to physical restriction of the lungs' capacity to insufflate, such as chest wall injury, pneumo/hemo/chylothorax, or pleural effusion. It can also be the result of fibrosis of the lungs that occurs during the recovery phase from acute lung injury, such as radiation or drug injury, or pulmonary infarction secondary to pulmonary vascular disease, such as occurring with sickle cell disease. Fibrosis can also be caused as the result of chronic inflammation, such as is caused by some collagen vascular diseases.

Reversible Shunting

Reversible shunting may occur with atelectasis, which can result from mucus plugging, foreign body aspiration, and asthma. It can also occur in lobar pneumonia and pulmonary hemosiderosis. Chronic shunting can occur on the cardiac level, or the pulmonary level, via AVMs, which can be either congenital or acquired, such as in the case of the hepatopulmonary syndrome.

Diffusion Defects

Diffusion defects, stemming from ILD, can be acute processes, such as in the case of infectious pneumonitis, caused by viruses, fungi, or PCP, hypersensitivity pneumonitis, or chronic aspiration. Acute ILD can also be caused by radiation or drug injury. Pulmonary edema, which can be caused by a number of mechanisms, such as cardiogenic, neurologic, or postobstructive, will also reduce diffusion capacity and thus lead to tachypnea.

Normal Growth and Physiology

2

Andrew A. Colin and Dennis Rosen

Overview of Respiratory Physiology

In analyzing a chest radiograph, it is important to have an understanding of some of the basic principles of respiratory physiology and to appreciate how certain pathophysiological processes can cause distinct disease states, each with its own specific clinical signs and symptoms [1, 2]. These can be divided into broad categories, which include obstructive lung disorders, restrictive lung disorders, disorders of gas diffusion, shunts, and ventilation-perfusion abnormalities. The following is a short overview of the physiologic considerations of these complex disorders. For more detail, the reader is advised to refer to the references below.

Obstructive Lung Disorders

Obstructive lung disorders affect the conducting airways and result from increased resistance to airflow within the airways and/or increased compliance of the airways. These disorders can be diffuse or localized. They can be caused by the presence of congenitally narrowed bronchi, scarred bronchi (such as in postinfectious bronchiolitis obliterans), intraluminal lesions, debris, or secretions (such as in acute bronchiolitis), dynamic airway wall changes leading to increased resistance to airflow as seen with bronchoconstriction or increased compliance as is seen in bronchomalacia or bronchiectasis, and extraluminal compression by a blood vessel or mass. Depending upon which segment of the conducting airways the obstruction is located in, the mechanism involved, and its severity, different phases of the respiratory cycle can be affected. Extrathoracic obstruction primarily causes problems in the inspiratory phase (stridor), though the expiratory phase can be affected as well, and intrathoracic obstruction will cause predominantly expiratory abnormalities (though here too, the wheezing, inspiratory phase can be affected). The underlying mechanism of this variable behavior is that during inspiration, negative intrathoracic pressure is generated by the inspiratory muscles, drawing air and the walls of the extrathoracic airways inward while the intrathoracic airways expand. During expiration, positive pressure is generated within the chest, propelling air outward, narrowing the intrathoracic airways lumina, and expanding the extrathoracic airways. When intrathoracic obstruction is significant enough to cause inhomogeneity in the rate of emptying in some or many parts of the lung, the chest radiograph shows hyperinflation and air trapping. Examples of common diffuse obstructive lung disorders include asthma, cystic fibrosis (CF), bronchiolitis obliterans, bronchiectasis, and bronchopulmonary dysplasia. A bronchial foreign body represents a localized obstructive defect. Spirometry, which measures airflow, can quantify the degree of obstruction and is the standard pulmonary function test.

Restrictive Lung Disorders

Restrictive lung disorders occur when the lungs are unable to inflate to normal volumes. They can occur with congenital or acquired loss of lung mass (e.g., agenesis of the lung or lobectomy/pulmonectomy, respectively) and parenchymal abnormalities, such as interstitial lung disease (idiopathic or secondary to an underlying disorder, such as a surfactant protein deficiency). They can also be caused by a musculoskeletal or neuromuscular abnormality which prevents the chest wall from expanding to full capacity during a maximal inspiratory effort. Examples of this type of restrictive process include congenital myopathies and neuromuscular disorders (such as spinal muscular atrophy) and more rarely diseases affecting the diaphragm. Bony chest wall abnormalities (such as thoracic dysplasia and scoliosis) inhibit lung

A. A. Colin
Miller School of Medicine, University of Miami, Miami, FL, USA

D. Rosen (✉)
Division of Pulmonary Medicine, Boston Children's Hospital and Harvard Medical School, Boston, MA, USA
e-mail: Dennis.Rosen@childrens.harvard.edu

R. H. Cleveland, E. Y. Lee (eds.), *Imaging in Pediatric Pulmonology*, https://doi.org/10.1007/978-3-030-23979-4_2

growth and expansion, as do intrathoracic space occupying processes (such as a diaphragmatic hernia, large pleural effusion, or tumor). The chest radiograph may show reduced lung volumes, albeit this may be difficult to pick up in the young child with a limited inspiratory effort. More obvious are distorted or bell-shaped chest walls (e.g., Jeune syndrome), scoliosis, or an abnormally diffuse parenchymal process, depending upon the underlying disorder. Physiologic assessment of these disorders is made by thoracic gas volumes measurement using plethysmography and gas (e.g., helium) dilution methods to quantify fractional lung volumes and assess the degree of restriction and measurement of maximal respiratory muscle pressures to assess muscle weakness. With a few exceptions, these methods require patient cooperation and are therefore limited in the young child. While the regular chest radiograph has limited value for quantification of restriction, algorithms exist to assess lung volumes using chest computed tomography (CT) scans.

Gas Diffusion Disorders

Gas diffusion disorders affect the absorption of oxygen into the bloodstream with resulting hypoxemia. This typically occurs due to a structural abnormality or thickening of the alveolar wall through which the gas exchange between the alveolus and the adjacent capillary occurs, resulting in hampered gas exchange. This can be seen in disease states such as interstitial lung diseases and pulmonary fibrosis. Gas diffusion disorders may present symptomatically with dyspnea upon exertion or at rest, tachypnea, and/or hypoxemia. The chest radiograph often shows an abnormally diffuse parenchymal process. Measurement of the diffusion capacity of the lung with carbon monoxide (DLCO) is diagnostic.

Ventilation Perfusion Mismatch and Shunt

Ventilation perfusion mismatching refers to a discrepancy between blood flow and aeration within a given lung unit. A greater perfusion-to-ventilation ratio is also known as a shunt and results in the return of unoxygenated blood to the left side of the heart and outward into the arterial blood stream, resulting in hypoxemia. The hypoxemia caused by shunts does not typically respond to the administration of oxygen, as the shunted blood does not come in contact with the supplemental oxygen, whereas the blood flowing through the other, normally perfused, lung units is already well-saturated. Fixed shunts can be seen with arteriovenous malformations, whereas intermittent shunting can occur with low lung volumes, retention of secretions, and in acute atelectasis. The chest radiograph may reveal the underlying pathology; however, vascular malformation in the lungs is usually elusive to the standard chest radiograph and requires more advanced radiologic modalities such as chest CT or MRI imaging. Intrapulmonary shunts are much less common than right-to-left shunts of cardiac origin and are typically addressed once an underlying cardiac abnormality has been ruled out.

A greater ventilation-to-perfusion ratio can occur in congenital disorders, such as the absent development of a pulmonary artery, or in intravascular processes such as a pulmonary embolism. The physiologic/clinical effect of these disorders that result in relative "wasted ventilation" or in the extreme dead-space ventilation is mild relative to shunt, in particular with the long-standing circumstances such as congenital vascular anomalies, often with absence or minor hypoxic effects. The common chest radiograph often is of limited diagnostic value. Thus, when a V/Q mismatch is suspected, a ventilation-perfusion scan may be useful, and, in cases where a pulmonary embolus is suspected, a CT with IV contrast can be diagnostic.

Lung Development and Effects on Lung Physiology

For the pediatric radiologist, lung mechanics and in particular those related to changes in lung volume are of crucial significance. One has to keep in mind that the radiograph of the noncooperative young child is rarely obtained at the optimal full inflation typical for the older person who inhales to full lung capacity (thus, total lung capacity or TLC) and breath-holds. The lung volumes reflected in the pediatric radiograph (assuming quiet breathing) span a volume range from functional residual capacity (FRC) (the volume at end expiration) to peak of tidal volume (the volume at end inspiration). Thus, by definition, the volume of the usual pediatric radiograph is almost always well below the lung volume of the cooperative patient, with all the implications that this has on the quality of the radiograph. Obviously, the lower the lung volume, the less reliable is the interpretation of pathology.

Stages of Lung Development

Early growth and development of the human lung is a continuous process that is highly variable between individuals and has traditionally been divided into five stages [3]. The first is the embryonic phase (26 days to 6 weeks of gestational age [wGA]), followed by the pseudoglandular (6–16 wGA) stage. At the end of this stage, the major elements of the bronchial tree complete their branching. The third is the canalicular stage (16–28 wGA). In the later phase of this stage, the prealveolar elements may allow infant survival. The saccular stage (28–36 wGA) is the one in which most premature infants are born and is followed by the alveolar (36 wGA–term) phase, which continues into childhood. The

saccular period, 28–36 wGA, is a transitional phase before full maturation of alveoli occurs. The primitive alveoli that become gradually more effective as gas exchangers have alveolar walls that are more compact and thicker than the final thin walls of alveoli; they also have an immature capillary structure. However, this partially developed structure is capable of carrying out a limited function of gas exchange that fully matures in the alveolar phase. Mature alveoli are not uniformly present until 36 wGA at which time the epithelium and interstitium decrease in thickness, air space walls proliferate, and the capillary network matures to its final single capillary network. Alveolar proliferation represents the predominant element of lung growth after birth. The alveolar proliferation rate is maximal in the first 2 years of life and subsequently decelerates. However, it is not well established to what age alveolar proliferation is maintained, and it may continue into later childhood or early adulthood.

The structural changes associated with the transition to mature alveoli through the alveolar stage and the following alveolar proliferation account for the subsequent gains in lung volume. Physiologically, these maturational changes not only affect gas exchange but together with the changes in the chest wall that will be discussed below have profound effects on the mechanical properties of the respiratory system and as such on the radiographic characteristics that are affected by these structural and mechanical considerations.

Changes in Lung Volume During the Last Trimester of Gestation

Calculations by Langston et al. [3] revealed that total lung volume undergoes rapid changes during the last trimester of gestation. At 30 wGA, the lung volume is only 34% of the ultimate lung volume at mature birth and at 34 weeks only reaches 47% of the final volume at maturity. In contrast, the air space (future alveolus) walls decrease in thickness such that at 30 and 34 weeks, they are 164% (28 μm) and 135% (23 μm), respectively, relative to the ultimate wall thickness at mature birth (17 μm). In parallel, dramatic increases in air space surface area occur. Surface area increases from 1.0–2.0 m^2 at 30–32 wGA to 3.0–4.0 m^2 at term. These volume changes likely have direct mechanical implications in reducing the vulnerability caused by a low and unstable FRC. Maturation of the alveolar network improves parenchymal elastance and therefore airway tethering.

Functional Residual Capacity (FRC) Tends to Be Low and Unstable in Infancy

Maintenance of a stable and adequate functional residual capacity (FRC) is important to secure effective gas exchange. FRC is determined by the balance between the opposing forces of the chest wall and lung and is thus a direct function of their respective mechanical properties. In early life, a compliant chest wall offers little outward recoil to the respiratory system, and thus the elastic characteristics of the respiratory system approximate those of the lung. The lung is also more compliant (i.e., has less elastance) in premature and newborn infants. The lung becomes less compliant (i.e., increases in elastance) as it undergoes alveolization, and the interstitial network becomes more intricately woven. (*Note*: the interstitium here represents the alveolar wall; a different concept from the same term utilized in radiology.) Compliance of the chest wall is extremely high in premature infants and undergoes rapid stiffening in late intrauterine life [4], but this stiffening (or decline in compliance) continues over the first 2 years of life [5]. Therefore, in early life (and more so in premature infants), the almost absent elastic recoil of the chest wall leads to a lung–chest wall equilibrium that results in a mechanically determined FRC that is low relative to older children and adults.

Thus, the baseline FRC in the young infant tends to drive itself to low volumes because of the mechanical characteristics discussed above. To circumvent this limitation, infants, unlike older children, actively elevate their end-expiratory volume (EEV), to a level that is higher than the mechanically determined FRC. At least three mechanisms are involved in the protection of a high end-expiratory volume: (a) a timing mechanism that initiates inspiration at an end-expiratory volume above that determined by the mechanical properties of the chest wall and lung [6], the other two mechanisms modulate the expiratory flow; (b) laryngeal braking during tidal expiration, a variable resistor mechanism [7]; and (c) persistence of inspiratory muscle activity into the expiratory phase [8].

The age at which transition to an *adult* pattern and cessation of these series of protective mechanisms has not been established for all of them, but based on one study [9], they persist at least into late in the first year and into the second year of life. It is likely that for a premature infant, the transition may be delayed. Interference with these active protective mechanisms, such as apnea or sedation, immediately drives the system toward low lung volumes. Also to be kept in mind is that the infant's sleeping state, supine position, and REM sleep (predominant in infancy) all substantially reduce lung volumes [10].

Airway Tethering

An additional crucial mechanism that secures airway patency and thus adequate maintenance of FRC is airway tethering. Tethering is the mechanism coupling lung volume to airway patency and is mediated through the elastic components in alveolar walls that surround bronchi. These elastic fibers are anchored to each other creating an extended mesh that exerts

a circumferential pull on the intraparenchymal airways. This complex elastic network that in its entirety reflects the elastic recoil of the lung transmits tension from the pleural surface to individual bronchi; thus, tethering links (couples) lung volume changes to airway caliber. The tension oscillates with the inspiratory cycle and increases during inspiration, increasing airway caliber. The cross-sectional area of the airway decreases with decline in lung volume, and airways may close if the lung volume is driven to critically low ranges of FRC (as may occur through the processes described in the previous segment). Tethering of airways was shown to be absent or less effective in young experimental animals [11] and most likely in infants in whom alveolization and the associated parenchymal elastic network are still in early stages of development. The effect of reduced tethering is decreased airway stability, increased tendency to airway closure, increased airway resistance, and, ultimately, a tendency to collapse alveolar units in the lung periphery.

Lessons for the Pediatric Radiologist

With the above observations, the radiologist needs to keep in mind that the predictable deficiencies in lung volume in infants and in particular when interference occurs with the mechanisms that protect lung volume (e.g., sedation) have an immediate effect on the quality of imaging. Chest radiographs and in particular chest CT scans obtained at low lung volumes have artifactual "infiltrates" in the lung fields that result from closure of airways and atelectases. This occurs in particular in the periphery of the lung and in dependent areas of the lung that are subjected to gravitational effects. To overcome these effects inflation of the lungs during the acquisition of the imaging is desirable. Most attractive for this purpose is the methodology developed by Long and Castile [12].

Some further physiological concepts related to pediatric respiratory physiology may be of use to the pediatric radiologist. Lung emptying in expiration is under normal circumstances a passive maneuver. Expiratory flow rate is determined by the interplay between a force that expels the air from the lung and the properties of the airways through which this exhaled air traverses. This flow rate is termed the expiratory time constant (τ) and is indeed a product of the compliance of the respiratory system (C) and the resistance of the airways (R) (thus, $\tau = C \times R$). To clarify, the force driving the air out upon relaxation at end inspiration is the elastance of the respiratory system (combined elastic properties of the lung and chest wall); this term is the reciprocal of the previously discussed compliance. In other words, compliant structures such as the chest wall and the lung in the very young, as discussed above, offer little driving force in exhalation. Small airways, the patency of which is impaired because of relatively small lung volumes and insufficient tethering, offer relatively high resistance to flow. This may be complicated in conditions of uneven structures of airways and parenchyma, because of damage related to trauma to the lung, e.g., by mechanical ventilation, or infection, creating regions that offer uneven emptying profiles, or uneven expiratory time constants, bringing about inhomogeneity in lung emptying.

The need to protect lung volumes through the mechanisms described above results in a rapid breathing rate, short expiratory time, and absent expiratory pauses (rapid transition from expiration to inspiration). In such circumstances, when the breathing rate increases (for reasons such as hypoxia, fever, or infection), there may be insufficient time for full lung emptying, in particular when emptying inhomogeneity is present. This may result in air trapping and a radiological interpretation of *hyperinflation*. While no systematic studies exist on the duration of this phenomenon, it is likely to resolve within the second year of life when the maturational processes bring about a shift to the "adult" pattern of breathing.

References

1. Bryan AC, Wohl ME. Respiratory mechanics in children. In: Macklem P, Mead J, editors. Handbook of physiology, Sect. 3, Vol. 111: Part 1: Mechanics of Breathing, Chap. 12. Bethesda: American Physiological Society; 1986.
2. West JB. Respiratory physiology: the essentials. 8th ed. Philadelphia: Lippincott Williams & Wilkins; 2008.
3. Langston C, Kida K, Reed M, et al. Human lung growth in late gestation and in the neonate. Am Rev Respir Dis. 1984;129(4):607–13.
4. Gerhardt T, Bancalari E. Chestwall compliance in full-term and premature infants. Acta Paediatr Scand. 1980;69(3):359–64.
5. Papastamelos C, Panitch HB, England SE, et al. Developmental changes in chest wall compliance in infancy and early childhood. J Appl Physiol. 1995;78(1):179–84.
6. Kosch PC, Davenport PW, Wozniak JA, et al. Reflex control of expiratory duration in newborn infants. J Appl Physiol. 1985;58(2):575–81.
7. Kosch PC, Hutchinson AA, Wozniak JA, et al. Posterior cricoarytenoid and diaphragm activities during tidal breathing in neonates. J Appl Physiol. 1988;64(5):1968–78.
8. Mortola JP, Milic-Emili J, Noworaj A, et al. Muscle pressure and flow during expiration in infants. Am Rev Respir Dis. 1984;129(1):49–53.
9. Colin AA, Wohl ME, Mead J, et al. Transition from dynamically maintained to relaxed end-expiratory volume in human infants. J Appl Physiol. 1989;67(5):2107–11.
10. Henderson-Smart DJ, Read DJ. Reduced lung volume during behavioral active sleep in the newborn. J Appl Physiol. 1979;46(6):1081–5.
11. Gomes RF, Shardonofsky F, Eidelman DH, et al. Respiratory mechanics and lung development in the rat from early age to adulthood. J Appl Physiol. 2001;90(5):1631–8.
12. Long FR, Castile RG. Technique and clinical applications of full-inflation and end-exhalation controlled-ventilation chest CT in infants and young children. Pediatr Radiol. 2001;31(6):413–22.

Normal Pediatric Chest and Role of Advanced Imaging

3

Monica Kahye Johnson, Pallavi Sagar, and Robert H. Cleveland

The Normal Chest Radiograph and Clues to Cardiovascular Disease

Patients with respiratory and cardiovascular diseases often have overlapping symptoms. One of the first tests for patients with respiratory distress is a chest radiograph, which can frequently distinguish between primary lung disease and congenital heart disease.

The purpose of this chapter is to understand the appearance of a normal chest radiograph and which abnormalities point to cardiovascular disease. This chapter provides a simple approach to chest radiography and to distinguish patients with cardiovascular disease as the cause of their respiratory symptoms so that further appropriate testing can be performed.

We recommend a standard approach in evaluating a chest radiograph:

- Technical adequacy
- Cardiac chamber enlargement
- Pulmonary vascularity
- Situs and side of aortic arch
- Lung parenchyma
- Extra-cardiovascular structures

If the heart is enlarged or abnormally shaped, as well as there is abnormal pulmonary vascularity, pulmonary edema, pleural effusions, or an abnormally positioned aortic arch, then the patient may have a congenital or acquired cardiovascular disease. More importantly, a normal chest radiograph does not exclude congenital heart disease. Parenchymal abnormalities due to primary pulmonary disease are discussed in detail in other chapters.

M. K. Johnson (✉) · P. Sagar
Department of Radiology, Harvard Medical School and Massachusetts General Hospital, Boston, MA, USA
e-mail: mjohnson86@partners.org

R. H. Cleveland
Department of Radiology, Harvard Medical School, Boston Children's Hospital, Boston, MA, USA

Technical Adequacy

In infants, the frontal radiograph is frequently taken recumbent and in the AP (anterior–posterior) projection, while in older children, the film is obtained upright and in the PA (posterior–anterior) projection. In an optimal chest radiograph, the intervertebral disc spaces should be seen through the cardiomediastinal silhouette. An underexposed film (one that is too bright) may suggest pulmonary edema or pneumonia where it does not exist. On the contrary, an overexposed film (one that is too dark) may cause the interpreter to miss findings particularly in the lung parenchyma. These were common issues in the past, as radiographs were generated using screen film radiography. With the advent of digital radiography, which allows for post-processing, images which originally were improperly exposed may be remedied without re-exposing the child to ionizing radiation [1].

Patient motion, rotation, and angulation may also distort an otherwise normal appearing chest. In a well-centered film, the distance of the medial ends of the clavicles should be equidistant from the adjacent posterior spinous process. The anterior ribs should be equidistant from the lateral margins of the spine and posterior spinous processes of the vertebra. On the lateral view, there should be a very small distance between the posterior right and left rib margins. A slight rotation to the left may cause the appearance of enlargement of the left superior mediastinum and left cardiac structures. Conversely, right mediastinal and cardiac structures appear larger when the patient rotates to the right. A lordotic image can exaggerate the size of the cardiac apex.

The degree of inspiration should be assessed on every radiograph. Although the degree of inspiration can be measured indirectly, the amount of inspiration is best judged by experience. A good inspiratory image is one in which the anterior sixth or posterior eighth rib is visualized above the

R. H. Cleveland, E. Y. Lee (eds.), *Imaging in Pediatric Pulmonology*, https://doi.org/10.1007/978-3-030-23979-4_3

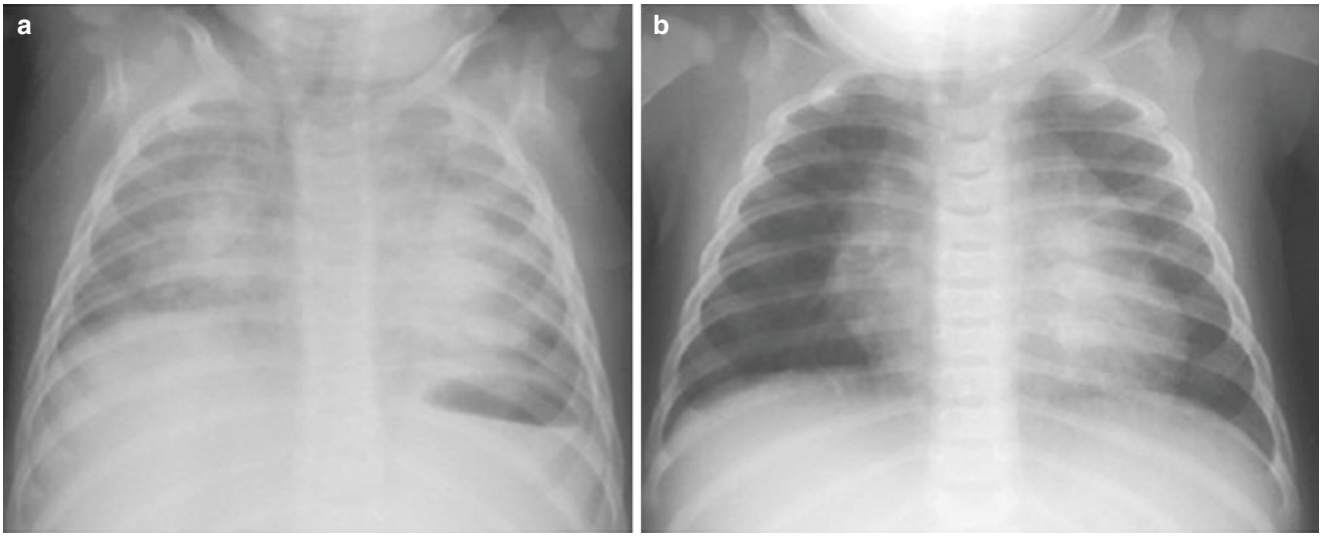

Fig. 3.1 (**a**, **b**) Expiratory and inspiratory radiographs with posterior rib fractures. These two frontal radiographs on the same patient emphasize the importance of lung volumes when interpreting a chest radiograph. The first frontal radiograph (**a**) is performed in expiration, as evidenced by low lung volumes, bilateral atelectasis, and tracheal deviation toward the right. The second radiograph (**b**) performed moments later in inspiration shows clear lungs and left posterior rib fractures in a patient with non-accidental trauma

apex of the left hemidiaphragm. In general, radiographs taken during expiration may show the dome of the left hemidiaphragm above this level. The lateral view and the appearance of flattened hemidiaphragms are also useful in determining the degree of inspiration. Many experienced radiologists rely on the degree of flattening of the diaphragm as the primary criterion of determining the degree of lung inflation.

Films obtained with very high lung volumes may produce an appearance of abnormal uplifting of the cardiac apex and thus be confused for right ventricular enlargement. Films obtained in expiration causes crowding of the normal bronchovascular structures and thus produce opacities suggesting edema, atelectasis, or pneumonia where it does not exist. Furthermore, these films may also obscure important lung parenchymal findings (Fig. 3.1a, b).

Normal Heart Size, Shape, and Position

In order to determine the size and position of cardiomediastinal structures, the appearance of the normal thymus must be understood. This is especially important in infants and toddlers where the normal thymus fills the anterior mediastinum and can obscure the superior cardiac border and mediastinum, the side and size of the great vessels, and the normal borders of the heart. Normally, the thymus involutes with increasing age and should be relatively inconspicuous by the end of the first decade.

The classic appearance of a newborn thymus is anterior superior mediastinal soft tissue that blends imperceptibly with the cardiac silhouette. A large thymus can simulate upper lobe atelectasis [2]. The other classic appearance is of the *sail sign*, which is more commonly seen on the right. The lateral edge of the thymus is often undulating, due to adjacent rib compression, *the thymic wave sign* [3]. On the lateral view, the thymus fills the anterior superior mediastinum and has a well-defined inferior border. Some of the different appearances of the thymus are pictured in Fig. 3.2.

There is a great variation in the size of the normal thymus [4]. The size varies during the respiratory cycle, e.g., inspiration (causing a small appearing thymus) and expiration (causing a larger appearing thymus). The thymus is also a dynamic organ and fluctuates in size during periods of prolonged illnesses. It may become smaller with infection or medications such as steroids or chemotherapeutic agents (stress atrophy) and rebound in size after recovery (rebound hypertrophy) [5–8]. A thymus may be pathologically enlarged if the enlargement persists into the second decade, if the borders are unusually lobular in contour, or if adjacent structures are displaced [9].

Both frontal and lateral views are necessary to adequately assess the position, shape, and size of the heart. On a well-centered frontal view of the chest, the normal heart and cardiac apex are centered to the left of the spine. From superior to inferior, the right cardiac margin is formed by the superior vena cava (upper one third) and right atrium (lower two thirds). The right atrium borders the right middle lobe. The ascending aorta is not normally seen in children. The soft tissue border of the superior vena cava often extends more laterally from the spine in young children than in adults.

The border of the left cardiomediastinal silhouette from superior to inferior is formed by the aortic arch (Fig. 3.3a,

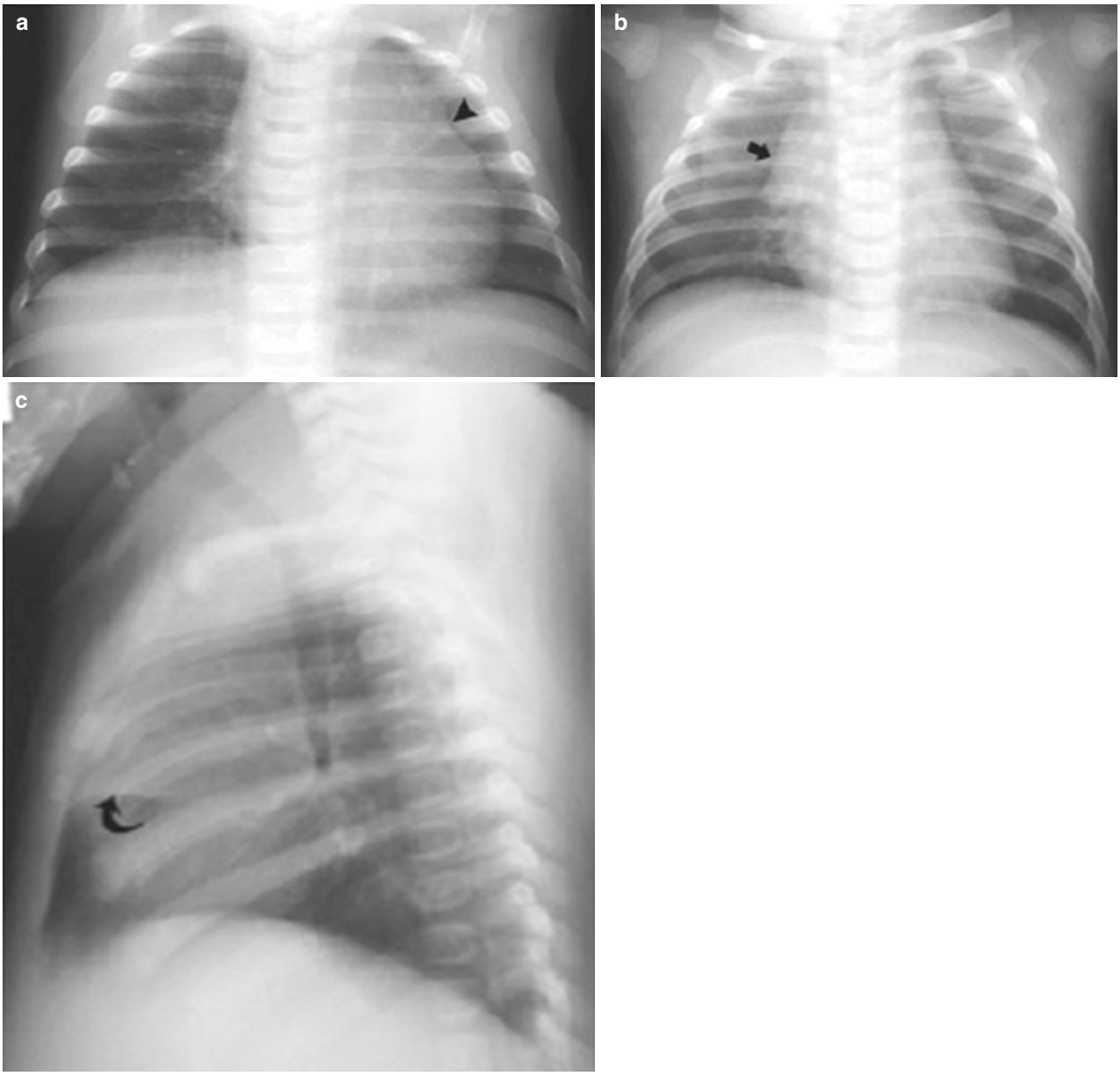

Fig. 3.2 (**a**–**c**) Normal thymus. These three images demonstrate the normal appearance of the thymus in infancy. The first image (**a**) demonstrates a thymus nearly completely filling the left upper chest with a smooth wavy contour (*arrowhead*) due to compression of the adjacent ribs. The thymus blends imperceptibly with the superior and lateral margin of the heart and superior mediastinum. The second image demonstrates the *sail sign* of the thymus. The thymus (*arrow*) blends in with the right superior cardiac and mediastinal borders and forms a sharp lateral border mimicking a sail. On the lateral view of the chest (**c**), the thymus fills the retrosternal clear space and has a sharply defined inferior margin (*curved arrow*)

arrowhead), main pulmonary artery (arrow), left atrial appendage (wavy arrow), and left ventricle (curved gray arrow). The left atrial appendage may not be seen in a normal heart. Normally, the borders of the left atrium and right ventricle do not contribute to the borders of the cardiac silhouette on the frontal view. The borders of the left atrium can be normally seen though the silhouette of the heart in 30% of children (Fig. 3.4, arrow) [10].

On the lateral view of the chest, the anterior cardiomediastinal border is formed (from superior to inferior) by the ascending aorta (arrowhead), main pulmonary artery (arrow), and right ventricle (curved arrow). The retrosternal clear space, or relatively lucent area cephalad to the right ventricle and posterior to the sternum, typically occupies one third to one half of the anterior chest (Fig. 3.3b). In infants, the thymus occupies the anterior mediastinum and may fill the

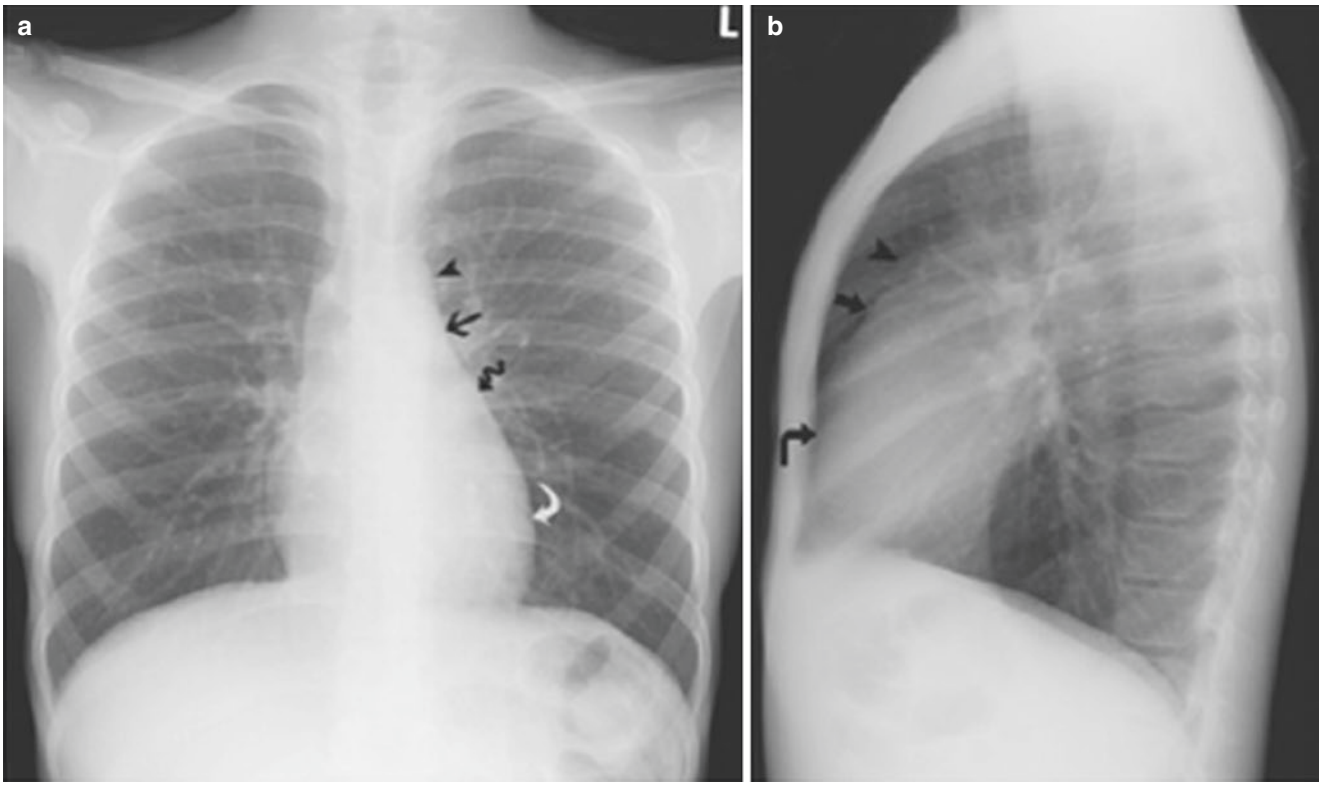

Fig. 3.3 (**a**, **b**) Normal PA and lateral radiographs of the chest in a 10-year-old

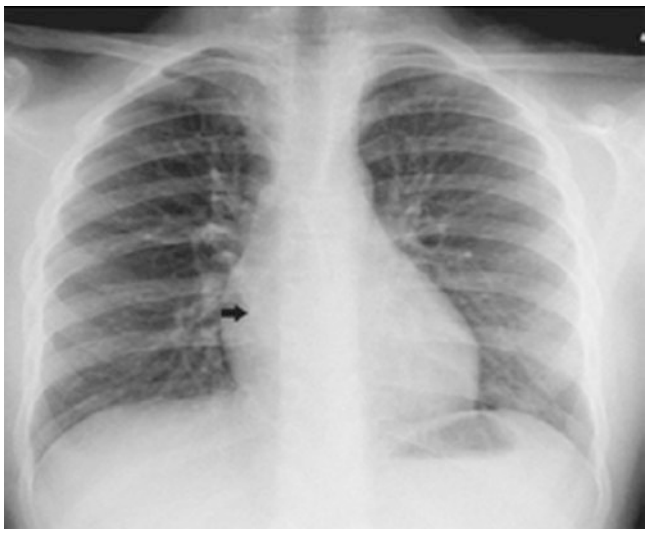

Fig. 3.4 Normal PA radiograph in a 10-year-old showing the normal left atrial shadow (*arrow*)

retrosternal clear space obscuring the anterior superior border of the heart and great vessels.

The posterior cardiomediastinal margin from superior to inferior is composed of the left atrium, left ventricle, and inferior vena cava on the lateral view. Normally, the posterior margin of the left atrium is anterior to the left mainstem bronchus and should not displace the bronchus or extend posterior to the inferior vena cava.

The normal heart size can be judged qualitatively and quantitatively. One index, the cardiothoracic ratio, is the ratio between the widest transverse cardiac diameter and the widest internal thoracic diameter. Normal values during quiet respiration are less than 60% for newborns and less than 50% for all children greater than 1 month of age [11, 12]. However, neither the left atrium nor the right ventricle is represented in the transverse dimension of the heart, making this measurement unreliable. Thus, a subjective evaluation of the heart size, based on the frontal and lateral views, with attention to each chamber of the heart and the overall cardiac size is preferred. Comparison to prior films is also valuable.

Judging heart size or specific chamber enlargement on an AP view of the chest in an infant with a large thymus is very challenging (Fig. 3.5a, b). The lateral view is particularly helpful. If the posterior aspect of the cardiac silhouette extends over the vertebral bodies, then the heart is enlarged. If the posterior margin of the heart extends posterior to the anterior line of the trachea, the heart may be enlarged. Another way of judging cardiomegaly is if the posterior border of the heart is closer to the anterior edge of the spine than the AP width of the adjacent vertebra.

Cardiac silhouette enlargement may be due to global chamber enlargement or due to specific chamber enlargement. Determining which chambers are enlarged provides clues to the type of cardiac abnormality. For example, global cardiac enlargement may be due to a cardiomyopathy or peripheral arterial to venous shunting due to tumors

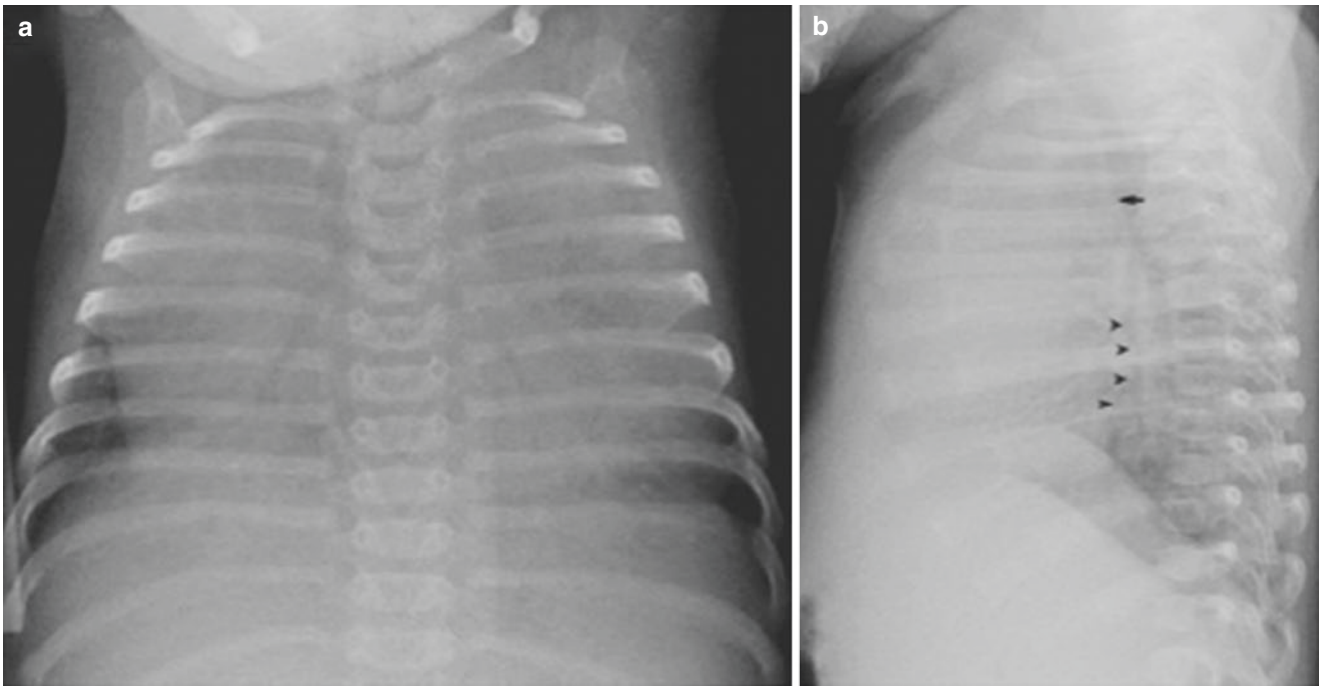

Fig. 3.5 (**a**, **b**) AP and lateral radiographs in an infant with a large central soft tissue which nearly opacifies both hemithoraces. The lateral radiograph demonstrates that the posterior margin of the heart (*arrowheads*) does not extend posterior to the anterior margin of the trachea (*arrow*). Ultrasound showed that this mass is a normal large thymus, and the heart was normal

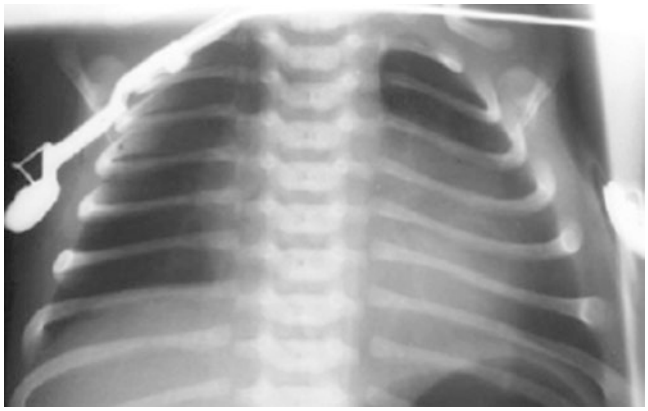

Fig. 3.6 Ebstein anomaly. This frontal view of the chest in an infant with Ebstein anomaly demonstrates an enlarged box-shaped cardiac silhouette due to a massively enlarged right atrium. The lungs appear hyperlucent because of decreased pulmonary blood flow

Fig. 3.7 Valvar pulmonary stenosis. This radiograph in a cyanotic infant demonstrates right ventricular enlargement as evidenced by an enlarged left cardiac margin in a patient with pulmonary valve stenosis. This image also demonstrates pulmonary vascular oligemia

(e.g., hemangioendothelioma) or vascular malformations (e.g., vein of Galen aneurysm).

The size and shape of the normal right atrium are variable; thus, mild to moderate enlargement of this chamber can be missed. Two signs of right atrial enlargement on the frontal projection are that the border is laterally displaced more than a few centimeters from the spine. When the right atrium is enlarged, the right heart border becomes squared, and the entire heart assumes a box-like appearance. The most common causes of right atrial enlargement in newborns are pulmonary atresia with an intact septum or Ebstein anomaly (Fig. 3.6).

When the right ventricle is enlarged, the retrosternal clear space becomes smaller. When the right ventricle enlarges, there is a clockwise rotation of the heart, and the cardiac apex can point upward (Fig. 3.7). In infants and young children, evaluation of the right ventricle on the lateral view may be impossible due to the thymus.

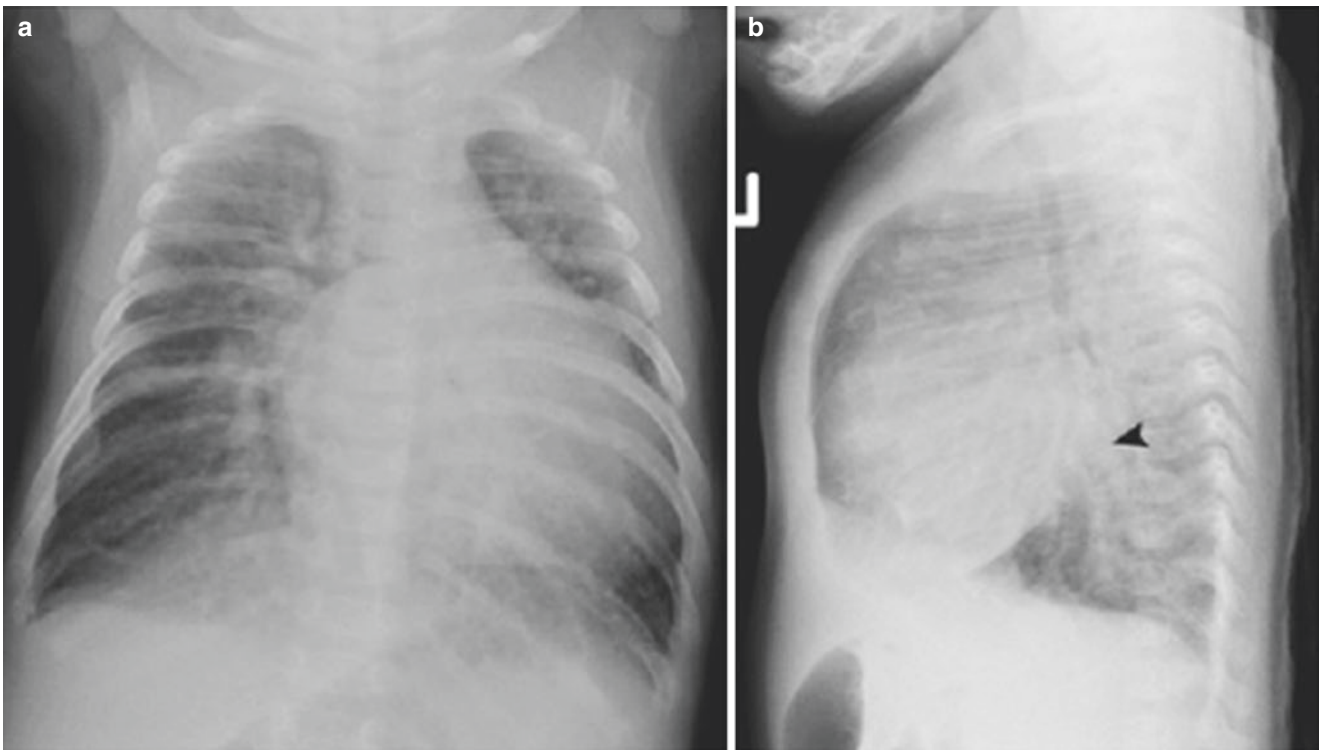

Fig. 3.8 (**a**, **b**) AV canal. Frontal and lateral views of the chest in a patient with trisomy 21 and an unrepaired AV canal defect demonstrate hyperinflation, cardiomegaly, and increased pulmonary vascularity. The lateral view shows left atrial enlargement as evidenced by the posterior margin of the left atrium (*arrowhead*) extending posterior to the inferior vena cava and pushing the left mainstem bronchus posteriorly. Notice that the angle between the left mainstem bronchus and axis of the trachea/right mainstem bronchus increases with left atrial enlargement

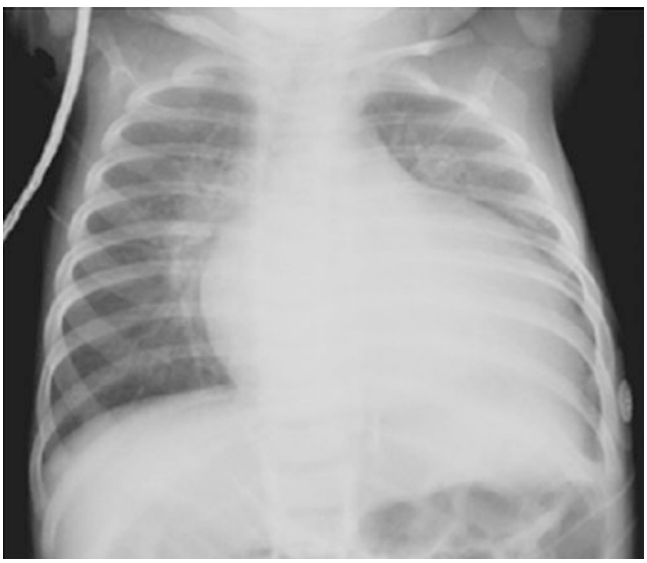

Fig. 3.9 Aberrant coronary artery. This infant presented to the ER with respiratory distress. The frontal radiograph demonstrates cardiomegaly, mainly due to left ventricular dilatation. The patient was found to have an aberrant left coronary artery arising from the left pulmonary artery on echocardiography

Left atrial enlargement is best seen on the lateral view. An enlarged left atrium extends posterior to the inferior vena cava and pushes the left mainstem bronchus posteriorly. In children, left atrial enlargement may be due to ventricular septal defect (Fig. 3.8a, b), patent ductus arteriosus, mitral stenosis, or mitral insufficiency.

Left ventricular enlargement is best seen on the frontal view and is demonstrated by enlargement of the left side of the heart. Left ventricular dilatation may produce a downward pointing cardiac apex. In this patient with an anomalous coronary artery (Fig. 3.9), both the left atrium and left ventricle were enlarged by echocardiography.

Vascular Pattern

Determining normal and abnormal pulmonary vascularity may be the most difficult aspect of evaluating a chest radiograph, but is very important to generating the appropriate diagnosis of congenital heart disease. Pulmonary vascularity can be normal and demonstrate increased pulmonary arterial flow, increased pulmonary venous distention, or decreased pulmonary flow. Normally, the right interlobar pulmonary artery is the same size as the trachea at the level of the aortic arch (Fig. 3.10).

The peripheral arteries normally taper gradually from the hilum to the periphery of the lung (see image normal PA of the chest). If the patient is upright, the width of the vessels in

Fig. 3.10 Normal diameter of the right interlobar pulmonary artery relative to the trachea. This magnified view of the chest demonstrates that the width of the normal right interlobar pulmonary artery (*arrowheads*) is the same as the trachea (*arrows*) at the level of the aortic arch. The spinal curvature allows the right hilar structures to be better visualized

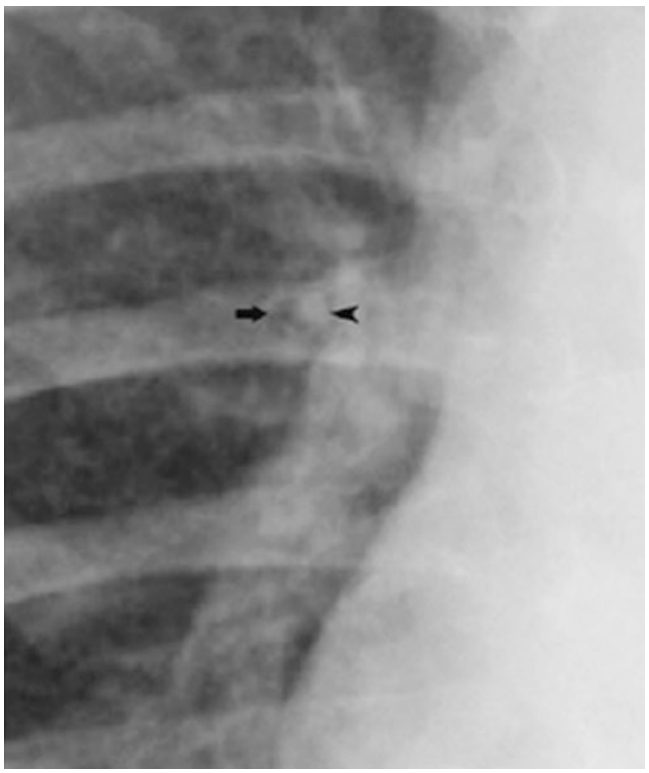

Fig. 3.11 Pulmonary artery on end with bronchus. This magnified view of the chest demonstrates a pulmonary artery (*arrowhead*) and adjacent bronchus (*arrow*) in cross section. Normally the diameter of these two structures is similar

the upper lobes is smaller than that of the lower lobes at comparable branch level. If the patient is recumbent, pulmonary vascular markings are more evenly distributed in size. Normally, the margins of the peripheral arteries (seen on end) are approximately the same size as the adjacent bronchi (Fig. 3.11). The borders of the peripheral arteries are normally sharp.

When pulmonary arterial flow is increased, the right interlobar artery will be larger than the trachea, and the apparent number and size of pulmonary arteries will increase. The pulmonary artery seen on end will be larger than the adjacent bronchus (Fig. 3.12). With increased pulmonary venous flow and edema, the margins of the enlarged vessels will become poorly defined. Increased pulmonary venous flow is often confused with peribronchial cuffing as seen in viral pneumonia.

Decreased pulmonary vascularity reflects diminished pulmonary blood flow. The main pulmonary artery segment may be decreased in size, the blood vessels appear thin, and the sparseness of the vessels gives an appearance of hyperlucency of the lungs (Fig. 3.6, Ebstein anomaly).

The Side of the Aortic Arch and Situs

The aorta is normally to the left of the spine, cephalad to the main pulmonary artery. In children, the thymus often obscures direct visualization of the aorta, and the position of the aortic arch is inferred by the deviation of the trachea. The trachea deviates to the opposite side of the aortic arch, especially during expiration [13, 14]. (For an image, refer to the expiratory radiograph in the patient with rib fractures.)

A right aortic arch serves as a warning for the presence of congenital heart disease. In the general population, right-sided aortic arch is associated with congenital heart disease in 5% of patients, especially truncus arteriosus, tetralogy of Fallot (Fig. 3.13), and pulmonary atresia with ventricular septal defect [15]. Right-sided aortic arches may also indicate the presence of variant arch anatomy or a vascular ring, most commonly due to an aberrant left subclavian or double aortic arch [15, 16].

Situs refers to the position of the chambers of the heart and tracheobronchial tree relative to abdominal organs (the

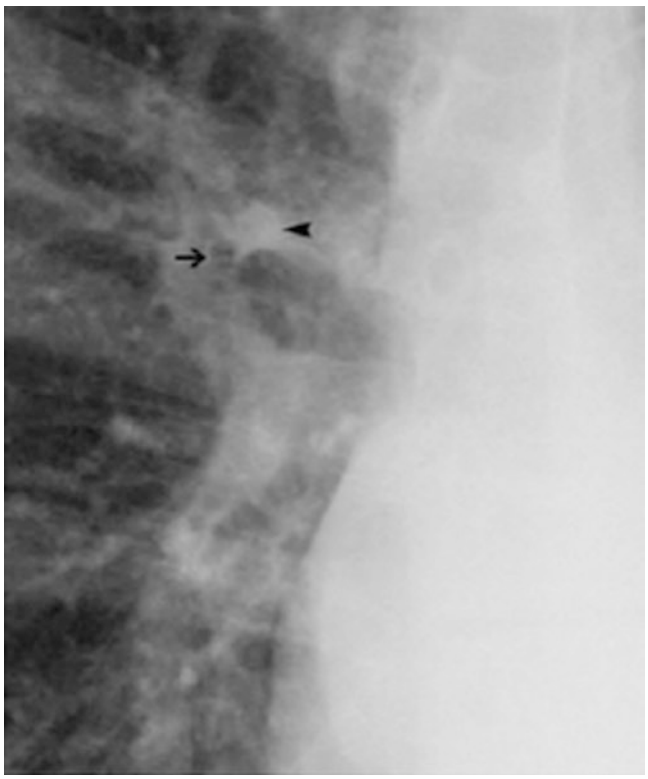

Fig. 3.12 Increased pulmonary arterial flow. A magnified view demonstrates that the pulmonary artery (*arrowhead*) is larger than the adjacent bronchiole (*arrow*). Increased pulmonary vascularity is also demonstrated in the previous patient with trisomy 21 and an AV canal

liver, spleen, stomach). Situs solitus is the normal position of the thoracic and abdominal organs, while situs inversus is its mirror image (i.e., the heart on the right, the liver on the left). Levocardia is when the heart points to the left chest (normal anatomy), while dextrocardia is when the heart points toward the right. The importance of situs and the position of the heart is that there is an increased incidence of congenital heart disease in patients with situs abnormalities. The frequency of congenital heart disease in patients with normal anatomy is 1%. In patients with situs solitus and dextrocardia or situs inversus and levocardia, the incidence of congenital heart disease approaches 100%.

Practically speaking, the cardiac apex, stomach, and spleen should be on the left, and the liver should be centered in the right upper abdomen. If there is discordance between the location of the cardiac apex and the gastric bubble, there is a very high incidence of congenital heart disease.

Extra-cardiovascular Structures

Pleural

Cardiovascular disease is one of the many causes of pleural effusions. On the standard PA and lateral chest radiographs, the costophrenic angles should be well visualized and sharp. The lateral view is the most sensitive view of detecting effusions and is represented by blunting of the costophrenic sulci. A lateral decubitus view may be sensitive for showing effusions and if large effusions are free flowing or loculated. Fluid may also track along the fissures so that the fissures appear thickened.

Fig. 3.13 Tetralogy of Fallot with right aortic arch. This radiograph in a patient with tetralogy of Fallot demonstrates a right aortic arch and enlarged upturned cardiac apex. The appearance of the heart is due to an enlarged right ventricle which causes clockwise rotation of the heart. There is decreased pulmonary vascularity, due to subpulmonic stenosis with a ventricular septal defect allowing a right to left shunt

Diaphragm

The heights of the two hemidiaphragms vary somewhat from person to person and with positioning. The relative heights of the two hemidiaphragms may also vary. It has been suggested that in normal individuals, the right may be as much as 0.5–2 intercostal spaces higher than the left and that the left may be up to 0.5 interspace higher than the right [17].

Bony

Certain bony findings on a chest radiograph may also point to the presence of congenital heart disease. Scoliosis, particularly thoracic scoliosis, can be associated with congenital heart disease [18]. Patients with vertebral anomalies may also have the VATER association of anomalies, which include vertebral, anorectal, esophageal atresia, renal, or radial ray limb anomalies and congenital heart disease [19]. Inferior rib notching may be a very subtle sign of coarctation of the aorta and is mainly seen in older children. Eleven pairs of ribs or multiple manubrial ossification centers are seen in patients with Down syndrome who also have an increased incidence of congenital heart disease [20]. Thoracotomy changes, median sternotomy wires, and vascular coils may give clues to prior cardiothoracic surgery. Lack of calcification of the inferior segments of the sternum, the mesosternum, may also be associated with congenital heart disease (Fig. 3.14).